Single Quantum Pair Annihilation And Its Contribution In The Calculation Of Photon Mass Energy Absorption Coefficients

By

Lutende Macleans Ndawana

A dissertation submitted to the University of Zambia

in partial fulfilment of the requirement of the degree

of Master of Science in Physics

THE UNIVERSITY OF ZAMBIA

LUSAKA

1997

I do solemnly declare that this dissertation represents my own work which has not been submitted for a degree at this or another university

Signature..

To my wife Daisy, my son Lweendo
and my daughter Lupo

This dissertation of Lutende Macleans Ndawana is approved as fulfilling part of the requirements for the award of the Master of Science Degree in Physics by the University of Zambia

EXAMINERS

1. Signature...................................Date...7/8/97

2. Signature...................................Date...2/8/97

3. Signature...................................Date.....................

4. Signature...................................Date.....................

ABSTRACT

This dissertation considers the single quantum pair annihilation of positrons with bound K-shell electrons in heavy atoms. It gives numerical calculations of the total cross section. By means of the method due to Basbas *et al.*[14], the binding-energy effect and its contribution to SQA cross sections is calculated. This calculation is done by use of a method suggested by Tseng and Pratt[6]. It is seen that at low positron energies the contribution due to binding-energy effect is significant. Recently Seltzer[13] has shown that the contribution of single quantum pair annihilation cannot be neglected in the calculation of photon mass energy absorption coefficients. Seltzer[13] included these contributions by means of an approximate analytical formula that tries to approximate the exact cross section calculations of Sheth and Swamy[10] and of Broda and Johnson[8]. This approximate analytical formula used by Seltzer[13] is seen to be inconsistent with the behaviour of the cross section as a function of energy. In this work we propose an improved analytical formula that can be used in the above calculations.

ACKNOWLEDGEMENTS

I am greatly indebted to my supervisor Professor C. V. Sheth, whose guidance and constant support has made this work possible. My sincere appreciation to Dr. H. V. Mweene for his constant support, guidance and encouragement.

My sincere thanks go to the entire staff of the Department of Physics, University of Zambia, for their support. My sincere thanks also go to the Climate research laboratory and library and Prof. P. C. Jain for allowing me to use their computer facilities.

Last but not least, I thank my wife Daisy for encouragement during my studies.

CONTENTS

CHAPTER 1

1.1 GENERAL INTRODUCTION

The inverse process to that of the creation of an electron-positron pair is the annihilation of a positron and an electron. According to the hole theory, this has to be understood as a transition of an electron from a positive energy state to a negative energy state. The energy that is given out in this process equals $2mc^2$, and may be emitted in the form of one, two or three photons.

Positrons are known to annihilate with electrons via more than one mechanism, the number of final state photons and their energy distribution being determined by the electron and positron quantum states. For an electron and a positron nearly at rest, two quanta of approximately $0.5mc^2$ each are emitted in opposite directions. Using the hole theory, Dirac[1] was the first to calculate the probability of annihilation of an electron at rest with a positron in motion.

Bethe[2] showed that the distribution of the two emitted photons can vary between two extremes. At one extreme, corresponding to annihilation of the electron and positron at rest, the two photons are emitted in opposite directions with equal energy. For arbitrary but finite electron and positron energy, conservation of momentum and energy determines the angle between the emitted photons. At the other extreme, corresponding to the annihilation of very high energy positrons, the photons are emitted in opposite directions, one with one-half the rest mass energy of the electron, the other “hard” photon with the remainder. Thus in this extreme, the hard photon has nearly all the energy of the process.

The dominant process of positron annihilation is the two-quantum annihilation (DQA) where positrons almost at rest annihilate with free electrons in the target material[3, 4]. Owing to momentum conservation, the process should result in the emission of at least two photons. But when a positron in flight annihilates with an electron tightly bound to an atom, only one photon is emitted in so-called single quantum annihilation (SQA). This is possible because the nucleus participates in the momentum conservation. This implies that the process of SQA has the highest probability of occurring in the K shell. The Born approximation[5] shows that the SQA cross section is proportional to Z^5; annihilation is therefore more probable for heavy elements than for light ones.

The necessity of strong interaction with the nuclear Coulomb field implies that SQA is most probable for atoms with high electron density in the nuclear vicinity, the interaction being strongest in this region. We expect SQA to be most probable for atomic K shells, with cross sections for higher shells diminishing as the mean radii of the shells increase. Broda and Johnson[8] calculated the cross section of SQA for several high-Z elements using relativistic Coulomb wave functions. Their results were in good agreement with those previously reported by Jaeger and Hulme[9]. Sheth and Swamy[10] pointed out that the contribution of L_I -shell bound electrons to the SQA cross section cannot be neglected. They found that the L_I -shell contribution was about 16% of the K-shell cross section.

The relative probabilities of the SQA process versus the two-quantum annihilation (DQA) process are of considerable experimental importance, and have been estimated theoretically. Fermi and Uhlenbeck[7] calculated the ratio for low-velocity positrons, using non-relativistic wave functions, and obtained a value of about 10^{-13}. Bethe[2] calculated the ratio in the Born approximation for positron kinetic energies from 0 to $100mc^2$, allowing for SQA with only K-shell electrons and DQA with any atomic electron. He found that the ratio is proportional to Z^4, is zero for positrons of zero velocity, and rises continuously with increasing energy to a fairly flat maximum in the range $2mc^2$ to $20mc^2$, resulting in a value of about 1/6 for lead and only about 10^{-5} for air. Later calculations of the cross section for SQA confirmed the vanishingly small probabilities for small positron velocities[9, 10, 21]. This very small probability for low positron velocity must be attributed to the repulsive force of the nucleus preventing the slow positron from getting into the region of tightly bound electrons where annihilation is possible.

Analytical calculations of SQA cross sections in the pure Coulomb potential have been carried out by several authors. Most of these calculations ignore all but the K-shell contributions and predict total cross sections as functions of atomic number and incident positron energy. Several involve approximate expansions in αZ[4, 12]. Besides, they ignore the effects of binding energy change on SQA cross sections. We discuss this effect in detail in Section 2.8.

Moroi *et al.*[12] have developed analytical expressions for the differential cross sections for arbitrary atomic shells, based upon modified Sommerfeld-

Maue positron wave functions, valid to one order in αZ beyond the leading term. Unfortunately the need for terms of higher order in αZ is apparent for high atomic numbers. They find that for $Z = 82$ the K-shell total cross sections become negative for energies less than $4.4mc^2$.

Exact calculations of SQA polarisation correlations are few. Johnson[11] studied the azimuthal asymmetry of emitted radiation for polarised positron beams. Sheth and Swamy[10] calculated the total left-right circular photon polarisation resulting from K-shell annihilation of longitudinally polarised positrons. Pratt[31] studied the high energy limit of the correlation of positron-photon helicities. Using Sommerfeld-Maue electron and positron wave functions Banerjee[32] obtained the polarisation correlation for the K-shell photoeffect and SQA.

Recently, Broda and Johnson[8] have theoretically investigated the SQA cross sections by taking into consideration the screening effect of orbital electrons. They have found that the screening corrections to the Coulomb K-shell cross sections are sizeable for large atomic numbers and low for low positron energies, and that the ratio of L- to K- shell total cross section is significant for heavy atoms.

Exact relativistic calculations of SQA cross sections for K-shell electrons have been performed for several heavy elements[21]. In these calculations the wave functions in a point-Coulomb field were used for both the K-shell electron and the incident positron. However, Broda and Johnson[8] estimated the K and L shell SQA cross sections using wave functions that take into account screening effects for high-Z elements.

Pair production and the atomic photoelectric effect are characterised by distances which are small on the atomic scale, but large on the nuclear scale. In this case, wave functions in the atomic potential have a point-Coulomb form and the screening effect can be taken into account by a change in the normalisation of the electron wave functions in bound and continuum states. Tseng and Pratt[6] applied their model (the normalisation screening theory)[20] to SQA and found good agreement with the results of Broda and Johnson[8].

The use of a point-Coulomb model relies on the expectation, based on form-factor estimates, that atomic-electron screening effects are small. Lengthy relativistic calculations by Broda and Johnson[8] for SQA K- and L-shell cross sections in a screened potential for elements Z = 47 - 90 and positron energies 1.25, 1.50 and 1.75mc^2 have shown that atomic screening is not small for low positron energies and tends to increase the cross section at such energies.

The influence of electron screening can be considered to be the result of two opposing effects. One is the effective reduction of the nuclear charge, tending to reduce the SQA cross section, the other being an inhibition of the Coulomb repulsion of the positron, tending to increase the SQA cross section[8].

The present work will study SQA in the low energy regime. We shall consider SQA in the most simple case, where the electron is bound to the K shell of an atom and where the kinetic energy of the positron is large compared to the ionisation energy of the K shell. We shall derive an approximate closed formula for SQA. This derivation will be based on numerical procedures and on the already existing analytical and numerical results[5, 6, 8, 12, 13]. This is discussed in detail in Section 2.6.

Experimental studies of SQA are few. These investigations generally are concerned with experimental verification of the occurrence of SQA and with the determination of the dependence of the total cross section on the incident positron energy and atomic number of the target. Indeed, as was shown by Bethe[2], as the incident positron energy increases, the fractional difference in energy between the SQA photon and the hard DQA photon decreases, making experimental distinction between these two photons difficult. Recently experiments[22] have provided the first experimental data on the distributions of the annihilation radiation for the three major shells L, K and M.

We now discuss the relationship between the atomic photoeffect and the SQA. Their formal relationship is illustrated by the typical Feynman diagrams as shown in Figure 1.1 and Figure 1.2. In these figures, a bound electron of energy E_{nj} is represented by the double solid lines. p_- and p_+ are the energy momentum four-vector for the outgoing electron and the in-going positron, respectively. The Feynman diagram for the atomic photoeffect can be obtained from that for the SQA by the standard substitutions $p_+ \rightarrow p_-$, and $k \rightarrow -k$, which leave the energy-conservation law invariant. q is the momentum transferred to the nucleus and is negligible for most calculations.

Tseng and Pratt[6] exploit this relationship to apply their normalisation screening theory[18, 20], which is well developed with respect to the photoeffect, to single-quantum pair annihilation.

1.2 PLAN OF THE THESIS

This thesis is divided into five chapters. Chapter 2 deals with the theory of SQA and the effect of binding-energy change on the SQA cross section. A review of the topic of atomic-electron screening[6] and the derivation of an approximate analytical SQA formula are done in this chapter.

In Chapter 3 we discuss the attenuation coefficient and the mass energy-absorption coefficient. The contribution of SQA to the calculation of the photon mass energy-absorption coefficient is outlined in this chapter. Then in Chapter 4 we discuss the results of this work. Finally we give a conclusion in Chapter 5.

1.3 AIMS OF THIS WORK

The specific aims of this work are;

(a) to devise an approximate closed formula for the SQA (K-shell) cross section,

(b) to calculate the binding-energy change effect on the SQA cross section and to determine its dependence on the atomic number of the target element, and

(c) to calculate the contribution of SQA in the calculation of photon mass energy-absorption coefficients. This is done by calculating the contribution of SQA to the annihilation flight factor.

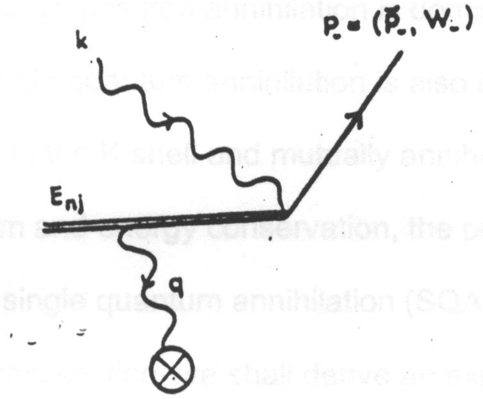

Figure 1.1: Feynman diagram for the atomic photoeffect.

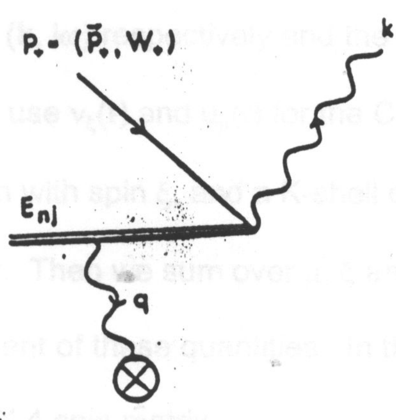

Figure 1.2: Feynman diagram for the SQA.

CHAPTER 2

2.1 DERIVATION OF THE SQA CROSS SECTION

Though positron annihilation is dominated by two-quantum annihilation (DQA), single quantum annihilation is also important. If the positron is able to penetrate to the K shell and mutually annihilates with an electron, then due to momentum and energy conservation, the process emits a single photon and results in single quantum annihilation (SQA).

In this section, we shall derive an expression for the SQA cross section. We shall follow closely the derivation of the K-shell cross section for SQA by Sheth[16] and by Johnson *et al.*[21].

Generally, the SQA cross section is given by

$$\sigma = \frac{\alpha W \omega}{4\pi p} \int d\Omega_k \sum_{\xi\varepsilon\mu} |M|^2 , \tag{2.1}$$

where M is a matrix element. M is given as

$$M = -i \int d^3 r \left\{ v_\xi^\dagger(\bar{r}) \bar{\alpha} \bullet \hat{\varepsilon}\, u_\mu(\bar{r}) \right\} \exp(-i\bar{k} \bullet \bar{r}) . \tag{2.2}$$

We have denoted the energy-momentum vectors of the positron and photon by (**p**, iW) and (**k**, iω) respectively and the photon polarisation vector by the unit vector $\hat{\varepsilon}$. We use $v_\xi(r)$ and $u_\mu(r)$ for the Coulomb-field Dirac wave functions for a positron with spin ξ, and a K-shell electron with magnetic quantum number μ respectively. Then we sum over μ, ξ and ε, since the observed cross sections are independent of these quantities. In the matrix element, equation (2.2), α is the Dirac 4 X 4 spin matrix.

In general the bound state wave functions for the electron can be written as[16]

$$u_\mu(r) = \begin{pmatrix} g_\kappa(k_b r)\chi_\kappa^\mu \\ if_\kappa(k_b r)\chi_{-\kappa}^\mu \end{pmatrix} \tag{2.3}$$

with $\mu = \pm\frac{1}{2}$.

Generally the radial functions g_κ and f_κ are given for any energy level in a point Coulomb potential as[41]

$$\left.\begin{matrix} g(r) \\ f(r) \end{matrix}\right\} = \pm \frac{(2\lambda)^{3/2}}{\Gamma(2\gamma+1)} \sqrt{\frac{E(1\pm E)\Gamma(2\gamma+n'+1)}{4(n'+\gamma)\left(\frac{(n'+\gamma)}{E}-\kappa\right)n'!}}(2\lambda r)^{\gamma-1}\exp(-\lambda r)$$
$$\times\left\{\left(\frac{(n'+\gamma)}{E}-\kappa\right)F(-n',\ 2\gamma+1;\ 2\lambda r)\mp n' F(1-n',\ 2\gamma+1;\ 2\lambda r)\right\} \tag{2.4}$$

where $n' = n - |\kappa|$, n is the principal quantum number, $\lambda = (1 - E^2)^{1/2}$, E is the eigenvalue of the Dirac equation in a Coulomb potential and F(a, c; x) is the confluent hyper-geometric function

$$F(a,\ c;\ x) = 1 + \frac{a}{c}x + \frac{a(a+1)}{c(c+1)2!}x^2 + \ldots.$$

For the K-shell, n = 1, l = 0, j = 1/2, n' = 0, and κ = 1.

The angular dependence in equation (2.3) is expressed by spherical spinors[29]

$$\chi_\kappa^\mu(\hat{r}) = \sum_\lambda C_{\mu-\tau,\ \tau,\ \mu}^{l\ \frac{1}{2}\ j}\, Y_l^{\mu-\tau}(\hat{r})\chi^\tau, \tag{2.5}$$

in which χ^{τ} are Pauli spinors, $C^{l\ \frac{1}{2}\ j}_{\mu-\tau,\ \tau,\ \mu}$ are the Clebsch-Gordan coefficients, $Y_l^m(\hat{r})$ are spherical harmonics, and in which

$$\kappa = \mp\left(j + \tfrac{1}{2}\right) \text{ for } j = l \pm \tfrac{1}{2},$$

and $\gamma = (\kappa^2 - (\alpha Z)^2)^{1/2}$.

The radial function $u_\mu(r)$ is normalised so that

$$\int_0^\infty r^2\left(g^2 + f^2\right)dr = 1, \tag{2.6}$$

and is a solution of the Dirac equation in a central potential $V(r)$

$$\left(\vec{\alpha}.\vec{p} + \beta + V(r)\right)u_\mu = E_b u_\mu . \tag{2.7}$$

In equation (2.7)

$$\vec{\alpha} = \begin{pmatrix} \vec{\sigma} & 0 \\ 0 & \vec{\sigma} \end{pmatrix} \text{ and } \beta = \begin{pmatrix} I & 0 \\ 0 & -I \end{pmatrix},$$

σ_i are the Pauli matrices, I is the 2 x 2 unit matrix and E_b is the K-shell binding energy. Equation (2.7) reduces to two coupled first-order differential equations in r:

$$\begin{aligned} \frac{dg}{dr} + \frac{(1+\kappa)}{r}g + \left(W + 1 - V(r)\right)f = 0, \\ \frac{df}{dr} + \frac{(1-\kappa)}{r}f - \left(W - 1 - V(r)\right)g = 0. \end{aligned} \tag{2.8}$$

The wave function v_ξ used to describe an incident positron of momentum **p** and spin projection ξ in the rest frame, which asymptotically approaches a plane wave plus an out-going spherical wave, is

$$v_\xi(\vec{r}) = 4\pi\sum_{\kappa m}(-1)^{\xi-\frac{1}{2}}\left(\chi_\kappa^{m^+}(\hat{p})\chi^{-\xi}\right)(-i)^{l-1}\exp(-i\delta'_\kappa)\begin{pmatrix} f_\kappa(pr)\chi_{-\kappa}^{m}(\hat{r}) \\ -ig_\kappa(pr)\chi_\kappa^{m}(\hat{r}) \end{pmatrix}, \tag{2.9}$$

and is obtained from the corresponding partial-wave decomposition of a continuum electron with momentum **p** and spin ξ by the familiar charge-conjugation procedure[33]. If $V(r)$ is some arbitrary central potential, f_κ and g_κ of equation (2.9) are then radial functions for an electron described by **p** and ξ, and are solutions of equation (2.8) with $V(r)$ replaced by $-V(r)$. The δ_κ' are the phase shifts for an electron in a potential $-V(r)$, and are given by[8]

$$\delta_\kappa' = \delta_\kappa + 1/2(l+1)\pi, \quad \delta_\kappa' = 0 \text{ for } V(r) = 0. \tag{2.10}$$

The normalisations of the radial functions g_κ and f_κ are such that their asymptotic forms are given by

$$g_\kappa(pr) \to \left(\frac{W+1}{2W}\right)^{\frac{1}{2}} \frac{\cos(pr+\delta'_\kappa)}{pr} \qquad pr \to \infty$$

and

$$f_\kappa(pr) \to \left(\frac{W-1}{W}\right)^{\frac{1}{2}} \frac{\sin(pr+\delta''_\kappa)}{pr} \qquad pr \to \infty. \tag{2.11}$$

2.2 EVALUATION OF THE MATRIX ELEMENT

In order to evaluate equation (2.2) we make use of the identity

$$\exp(i\bar{k}\bullet\bar{r}) = 4\pi\sum_{LM} i^L j_L(kr) Y_L^M(\hat{r}) Y_L^{M^*}(\hat{r}), \tag{2.12}$$

and the spherical-basis identities[29]

$$\vec{A} \bullet \vec{B} = \sum_{\lambda} A_{\lambda} B_{\lambda}^{*}$$
$$\sigma_{\lambda} \chi_{\kappa}^{\mu} = \sqrt{3} \sum_{\tau} C_{\tau,\lambda,\tau+\lambda}^{\frac{1}{2}\,1\,\frac{1}{2}} C_{\mu-\tau,\tau,\mu}^{l\,\frac{1}{2}\,j} Y_{l}^{\mu-\tau}(\hat{r}) \chi^{\tau+\lambda} \tag{2.13}$$

with λ = 1, 0, -1,

$$A_1 = -\left(A_x + iA_y\right)/\sqrt{2},\ A_{-1} = \left(A_x - iA_y\right)/\sqrt{2},\ \text{and } A_0 = A_Z. \tag{2.14}$$

When we substitute into equation (2.2) the matrix element becomes

$$\begin{aligned} M = (4\pi)^2 \int d\vec{r} \sum_{\substack{\kappa_1, m_1, \lambda \\ \tau, L, m}} \hat{\varepsilon}_{\lambda}^{*} j_L(kr) Y_L^{m^*}(\hat{r}) Y_L^{m}(\hat{k}) Y_{l_1}^{m+\xi^*}(\hat{p}) \sqrt{3}\, i^{-l-l_1} \exp(-\delta_{\kappa}^{\ *}) \\ \times C_{\tau,\lambda,\tau+\lambda}^{\frac{1}{2},1,\frac{1}{2}} C_{m_1+\xi,-\xi,m_1}^{l_1,\frac{1}{2},j_1} \{ f_{\kappa_1}^{*} f_{\kappa} C_{\mu-\tau,\tau,\mu}^{\bar{l}\,\frac{1}{2}\,j} C_{m_1-\tau-\lambda,\tau+\lambda,m_1}^{\bar{l}_1\,\frac{1}{2}\,j_1} Y_{\bar{l}_1}^{m_1-\tau-\lambda^*}(\hat{r}) Y_{\bar{l}}^{\mu-\tau}(\hat{r}) \\ - g_{\kappa_1}^{*} g_{\kappa} C_{\mu-\tau,\tau,\mu}^{\bar{l}\,\frac{1}{2}\,j} C_{m_1-\tau-\lambda,\tau+\lambda,m_1}^{\bar{l}_1\,\frac{1}{2}\,j_1} Y_{l_1}^{m_1-\tau-\lambda^*}(\hat{r}) Y_{l}^{\mu-\tau}(\hat{r}) \}. \end{aligned} \tag{2.15}$$

To simplify the notation we define the following integrals[8, 21]

$$I_{\kappa_1 L} = i^{-L-l_1} \exp(-i\delta_{\kappa}^{\ *}) \int_0^{\infty} r^2 dr \{ f_{\kappa_1}^{*}(pr) f_{\kappa_1}(kr) j_L^{*}(kr) \},$$
$$J_{\kappa_1 L} = i^{-L-l_1} \exp(-i\delta_{\kappa}^{\ *}) \int_0^{\infty} r^2 dr \{ g_{\kappa_1}^{*}(pr) g_{\kappa_1}(kr) j_L(kr) \}. \tag{2.16}$$

We then use the identity

$$\int d\Omega Y_{l_3}^{m_3^*}(\hat{r}) Y_{l_2}^{m_2}(\hat{r}) Y_{l_1}^{m_1}(\hat{r}) = \frac{[l_1][l_2]}{\sqrt{4\pi}[l_3]} C_{m_1\,m_2\,m_3}^{l_1\,l_2\,l_3} C_{0\,0\,0}^{l_1 l_2 l_3} \tag{2.17}$$

with the notation $[A] = \sqrt{2A+1}$.

Then the matrix element can be written as

$$M = (4\pi)^2 \sum_{\substack{\kappa_1, m_1 \\ L\lambda,\tau}} \sqrt{\tfrac{3}{4\pi}} \hat{\varepsilon}_\lambda^{\,*} Y_{l_1}^{m+\xi^*}(\hat{p}) Y_L^{\mu+\lambda-m}(\hat{k}) [L] C^{\frac{1}{2}\,1\,\frac{1}{2}}_{\tau,\ \lambda,\ \tau+\lambda} C^{l_1\,\frac{1}{2}\,j_1}_{m_1+\xi,\ -\xi,\ m_1}$$

$$\times \Big\{ \frac{[\bar{l}_1]}{[\bar{l}]} C^{\bar{l}_1\,L\,\bar{l}}_{0\,0\,0} C^{\bar{l}_1\,L\,\bar{l}}_{m_1-\lambda-\tau,\ \mu+\lambda-m_1,\ \mu-\tau} C^{\bar{l}\,\frac{1}{2}\,j}_{\mu-\tau,\ \tau,\ \mu} C^{l_1\,\frac{1}{2}\,j_1}_{m_1-\lambda-\tau,\ \tau+\lambda,\ m_1} I_{\kappa_1 L} \tag{2.18}$$

$$- \frac{[l_1]}{[l]} C^{l_1\,L\,l}_{0\,0\,0} C^{l_1\,L\,l}_{m_1-\lambda-\tau,\ \mu+\lambda-m_1,\ \mu-\tau} C^{l_1\,\frac{1}{2}\,j_1}_{m_1-\lambda-\tau,\ \tau+\lambda,\ m_1} C^{l\,\frac{1}{2}\,j}_{\mu-\tau,\ \tau,\ m_1} J_{\kappa_1 L} \Big\}.$$

The Racah algebra of equation (2.18) is considerably simplified for the K-shell where $\kappa = -1$, $l = 0$ and $\bar{l} = 1$. We square the matrix element, sum over μ, ξ and ε, then integrate over photon angles, using the identity

$$\sum_{\hat{\varepsilon}} \hat{\varepsilon}^*_\lambda \hat{\varepsilon}_{\lambda'} = \delta_{\lambda\lambda'} - \frac{k^*_\lambda k_{\lambda'}}{k^2}, \tag{2.19}$$

where $k_\lambda = k\sqrt{\frac{4\pi}{3}} Y_1^\lambda(\hat{k})$, and

$$\int \frac{k^*_\lambda k_{\lambda'}}{k^2} Y_L^m(\hat{k}) Y_{L'}^{m'^*}(\hat{k}) d\hat{k} = \tfrac{1}{3}\delta_{\lambda\lambda'}\delta_{LL'}\delta_{mm'} + (-1)^\lambda \frac{[L]}{[L']} C^{1\,1\,2}_{-\lambda,\ \lambda',\ \lambda'-\lambda} C^{112}_{000} C^{2\,L\,L'}_{0\,0\,0} C^{2\,L\,L'}_{\lambda'-\lambda,\ m,\ m'}. \tag{2.20}$$

We then obtain the formula for the total SQA cross section for the K shell:

$$\sigma = 16\pi\alpha \frac{W\omega}{p} \sum_{k=1}^{\infty} k \Big\{ |J_{k,k}|^2 + |J_{-k,k-1}|^2 + \frac{1}{(2k-1)} [(kI_{k,k} + (k-1)I_{k,k-2}) J^*_{kk} + \text{c.c.}]$$

$$+ \frac{1}{(2k+1)} [(kI_{-k,k-1} + (k+1)I_{-k,k+1}) J^*_{-k,k-1} + \text{c.c.}] + \frac{1}{(2k-1)^2} [(2k-1)^2 |I_{k,k}|^2 + 2k(k-1)|I_{kk-2}|^2$$

$$-(k-1)(I_{k,k} I^*_{k,k-2} + \text{c.c.})] + \frac{1}{(2k+1)^2} [2k(k+1)|I_{-k,k+1}|^2 + (2k^2-1)|I_{-k,k-1}|^2$$

$$+(k+1)(I_{-k,k-1} I^*_{-k,k+1} + \text{c.c.})] \Big\}. \tag{2.21}$$

The summation index k in equation (2.21) is related to the positron angular momentum by $k = j_1 + 1/2$. As the positron energy increases, more and more terms contribute to the sum. This decomposition is therefore most suitable for studying low-energy annihilation processes[21].

2.3 ANALYSIS OF THE RADIAL INTEGRALS

The radial integrals that we employ in the formulation are of the type

$$K = \int_0^\infty r^2 dr(2\lambda r)^{\gamma_1 - 1}(2pr)^{\gamma-1}\exp(-\lambda r - ipr)J_l(kr)F(a, b; 2ipr). \tag{2.22}$$

By use of a procedure due to Jaeger and Hulme[9] in the study of internal-conversion coefficients, we introduce an integral representation. The confluent hyper-geometric functions and the asymptotic series for the spherical Bessel functions are used to express the above integral in the form:

$$K = \frac{\Gamma(b)}{\Gamma(b-a)\Gamma(a)}\int_0^1 du\, u^{a-1}(1-u)^{b-a-1}[i^l \sum_{m=0}^{l} \frac{(-l, m)(l+1, m)}{(1, m)} i^{m+1} \int_0^\infty r^2 dr(2\lambda r)^{\gamma_1-1}(2pr)^{\gamma-1}(2kr)^{-m-1}$$
$$\times \exp(-\lambda r - ipr - ikr + 2ipru) + i^{-l}(k \to -k)]. \tag{2.23}$$

The r integral is written as a gamma function and the remaining parametric integral is expressed as a hyper-geometric function. The radial integral then reduces to

$$I_{\kappa l} = F_I \frac{\Gamma(\gamma - i\nu)\Gamma(\gamma+\gamma_1)}{\Gamma(2\gamma+1)}\kappa^\gamma \sum_{m=0}^{l} \frac{(-l,m)(l+1,m)}{(1,m)(1-\gamma_1-\gamma,m)} \frac{1}{y^m} \{[(\gamma - i\nu)F(\gamma_1 + \gamma - m, \gamma + 1 - i\nu;\ 2\gamma+1;\ \kappa)$$
$$+(\kappa - i\nu')F(\gamma+\gamma_1 - m, \gamma - i\nu;\ 2\gamma+1; \kappa)] + \exp(i\pi(\gamma+\gamma_1 - l - 1)\left(\frac{p+k-i\lambda}{p+k+i\lambda}\right)^{\gamma+\gamma_1-m}$$
$$[(\gamma - i\nu)F^*(\gamma+\gamma_1 - m, \gamma - i\nu;\ 2\gamma+1; \kappa) + (\kappa - i\nu')F^*(\gamma_1 - \gamma - m, \gamma+1-i\nu;\ 2\gamma+1;\ \kappa)]\}. \tag{2.24}$$

The integrals $J_{\kappa L}$ are obtained from equation (2.24) by replacing F_I by iF_J and changing $(k\text{-i}v')$ to $-(k\text{-i}v')$. In the previous equation we have

$$F_I = -N\left[\frac{1-\gamma_1}{2}\right]^{1/2}\left[\frac{W-1}{2W}\right]^{1/2}\exp\left(\frac{-i\pi\gamma_1}{2} - \frac{\nu\pi}{2z}\gamma_1 - 1\right)\frac{y}{8pk^2},$$
$$F_J = -N\left[\frac{1+\gamma_1}{2}\right]^{1/2}\left[\frac{W+1}{2W}\right]^{1/2}\exp\left(\frac{-i\pi\gamma_1}{2} - \frac{\nu\pi}{2z}\gamma_1 - 1\right)\frac{y}{8pk^2}, \tag{2.25}$$
$$\kappa = \frac{2p}{(p+k-i\lambda)},\ y = \frac{2k}{(p+k-i\lambda)},\ z = \frac{2\lambda}{(p+k-i\lambda)}.$$

Here $(l, m) = \Gamma(l + m)/\Gamma(l)$, $(-l, m) = (-1)^m l(l-1)\ldots(l - m + 1)$, $\nu = \alpha ZW/p$, $\nu' = \alpha Z/p$, $\gamma_1 = (1 - (\alpha Z)^2)^{1/2}$, $\lambda = \alpha Z$, and $N = [(2\lambda)^3/\Gamma(2\gamma_1 + 1)]^{1/2}$.

As an illustration of the above procedure Johnson *et al.*[21] used the Sommerfeld-Maue[29] wave functions for the bound state electron and plane waves for the positron, so as to obtain a closed form for the SQA cross section. Their numerical results agree well with the Born approximation formula in the limit Z tending to zero. The formula obtained by use of Sommerfeld-Maue wave functions is

$$\sigma(\varepsilon) = \frac{4\pi r_0^2 Z(Z\alpha)^4}{(\varepsilon^2 - 1)^{1/2}(\varepsilon + 1)^2}\left(\varepsilon^2 - \tfrac{1}{3}\varepsilon + \tfrac{4}{3}\right), \tag{2.26}$$

with ε being the energy of the positron in units of the electron rest mass. The actual cross-section calculation in equation (2.21) is performed numerically.

2.4 BOUND-STATE AND CONTINUUM-STATE WAVE FUNCTIONS WITH SCREENING

Broda and Johnson[8] have given a detailed numerical analysis of how screening is introduced into the calculation of the SQA cross section. In this section we shall follow their method. They introduce screening by use of numerical central potentials and bound-state wave functions predicted by the self-consistent relativistic Hatree-Fock-Slater (RHFS) atomic model. The potential used in solving equations (2.8), neglecting retardation effects, has the form[8]

$$V_{HFS} = -\left(\frac{\alpha Z}{r}\right) + V^{D}(r) - \overline{V}^{E}(r). \tag{2.27}$$

Here $\overline{V}^{E}$ is the average of the exchange-interaction term over all filled sub-shells according to the technique of Slater[36], and

$$V^{D}(r) = \frac{\alpha}{r}\left(\int_0^r n(r')dr' + r\int_r^\infty \frac{n(r')dr'}{r'}\right),$$

$$\overline{V}^{E}(r) = 3\alpha\left(\frac{3}{32\pi^2}\frac{n(r)}{r^2}\right)^{1/3} \tag{2.28}$$

with

$$n(r) = \sum_{\kappa}(2j_\kappa + 1)r^2\left(g_\kappa^2 + f_k^2\right).$$

The calculation of the total cross section, in equation (2.21), is essentially complete once the integrals $I_{\kappa L}$ and $J_{\kappa L}$ have been obtained. Because the potentials are not known analytically as a function of r, but only numerically, the calculation is done numerically. In all their calculations for bound-state wave functions Broda and Johnson[8] assume a point-Coulomb nucleus and they parametrise the potential in a Coulomb-like form

$$V(r) = -\frac{\alpha S(r)}{r}. \tag{2.29}$$

The function S(r) monotonically decreases with r and varies less rapidly for small r than V(r).

The integration of continuum-state wave functions g_κ and f_κ is done by a 10-point Lagrange integration scheme[8]. For the functions to remain bounded near r = 0, the integration for small r is carried out for G_κ, F_κ defined[8] by

$$g_\kappa(pr) = r^{\gamma-1}\, G_\kappa(pr),\quad f_\kappa(pr) = r^{\gamma-1}\, F_\kappa(pr) \tag{2.30}$$

with $\gamma = (\kappa^2 - (\alpha Z)^2)^{1/2}$. This transforms equations (2.8) into

$$\begin{aligned} \frac{dG_\kappa}{dx} &= -\frac{(\gamma+\kappa)}{x}G_\kappa - \left(\frac{W+1}{p} - \frac{\alpha S(r)}{x}\right)F_\kappa, \\ \frac{dF_\kappa}{dx} &= -\frac{(\gamma-\kappa)}{x}F_\kappa + \left(\frac{W-1}{p} - \frac{\alpha S(r)}{x}\right)G_\kappa, \end{aligned} \tag{2.31}$$

with $x = pr$, $S(r) \geq 0$ and W being in units of electron rest mass. The potential in equation (2.31), $V(r) = +\alpha S(r)/r$, is the sum of the nuclear-Coulomb and direct-interaction terms. Therefore

$$V(r) = -\left[-\left(\frac{\alpha Z}{r}\right) + V^D(r)\right]. \tag{2.32}$$

The average exchange-interaction term is omitted, since the incident positron has no exchange interaction with atomic electrons.

The phase shifts and normalisations used were calculated by parametrising the continuum-state functions G and F in a form similar to their asymptotic free-field limit as given by equation (2.11). The detailed discussion is given in reference 8. Once the numerical values for bound and continuum state wave functions are known, the radial-integral calculation is done through a numerical programme. In this case an eleventh-order closed type Newton-Cotes formula is used[8]. The screened SQA cross sections are obtained once the above calculation is done numerically.

2.5 SELTZER'S SQA CROSS SECTION

There are a number of papers dealing with SQA. For instance, Seltzer[13] and Moroi *et al.*[12] have derived analytical formulae for K-shell SQA cross sections. Unfortunately the formula given by Seltzer[13] gives negative cross sections for low and high positron energies, especially for high-Z values. The formula gives positive cross sections only for low-Z elements. This contradicts the theory of SQA, according to which the probability of SQA increases with the atomic number Z. However, the formula derived by Moroi *et al.*[12] agrees with most theoretical works, though it breaks down for Z > 82 and energies lower than $4.4mc^2$.

In an attempt to fit experimental and theoretical results, Seltzer[13] devised the analytic formula for the K-shell SQA cross section

$$\sigma(\mathrm{W}) = 4\pi r_0^2 \mathrm{Z}(\mathrm{Z}\alpha)^4 \beta \frac{\left(1 - \exp\left(-\frac{2Z\pi\alpha}{\beta}\right)\right)}{\left(1 - \frac{2Z\pi\alpha}{\beta}\right)} \frac{3\mathrm{W}^2 - \mathrm{W} + 4}{3(\mathrm{W}+1)^2(\mathrm{W}^2-1)^{1/2}}. \tag{2.33}$$

Here W is the energy of the positron in units of mc^2, r_0 is the classical electron radius, β is the speed of the positron divided by the speed of light and α is the fine structure constant. Equation (2.33) gives negative cross sections because the Coulomb factor in the denominator $2\pi\alpha Z/\beta$ is never less than unity for high atomic numbers. We believe this is due to a missing sign (the Coulomb factor should be written with a positive not a negative sign) and accordingly we have corrected the formula. Future references to this calculation are to be understood as incorporating this correction.

The result (2.33) is an improvement of the Born-approximation cross-section formula for SQA. The Born-approximation formula gives higher SQA cross-section values for the K shell. The formula is

$$\sigma(\mathrm{W}) = \frac{4\pi r_0^2 \mathrm{Z}(\mathrm{Z}\alpha)^4}{(\mathrm{W}^2-1)^{1/2}(\mathrm{W}+1)^2} \times \left[\mathrm{W}^2 + \frac{2}{3}\mathrm{W} + \frac{4}{3} + \frac{\mathrm{W}+2}{(\mathrm{W}^2-1)^{1/2}} \log\left\{\mathrm{W} + (\mathrm{W}^2-1)^{1/2}\right\}\right] \tag{2.34}$$

The symbols in equation (2.34) have the same meanings as those in equation (2.33). In the following sections we shall use the above equations

((2.33) and (2.34)) and the result derived by Moroi *et al.*[13] to devise a formula for the K-shell SQA cross section.

2.6 APPROXIMATION OF THE SQA CROSS SECTION

We use the Born-approximation equation (2.34) result for the K-shell total cross section in this derivation. The formula is modified by multiplying it by the so called 'Elwert factor'[17, 34]

$$f_E = \frac{\beta\left(1-\exp\left(\frac{-2\pi\alpha Z}{\beta}\right)\right)}{\beta'\left(1-\exp\left(\frac{-2\pi\alpha Z}{\beta'}\right)\right)} \tag{2.35}$$

In the formula, Z is the atomic number of the target element, α is the fine structure constant, β is the velocity parameter as defined in equation (2.33) and β' is the speed of the electron after interaction divided by the speed of light.

An expansion of the exponential in the denominator of equation (2.35) to first order and adding one in the denominator (to ensure the correct energy SQA cross section) leads to

$$f_{ME} = \beta\left(1-\exp\left(\frac{-2\pi\alpha Z}{\beta}\right)\right) \Big/ \left(1+\frac{2\pi\alpha Z}{\beta}\right). \tag{2.36}$$

We note that we have set $\beta = \beta'$ since the electron and positron mutually annihilate. The result has been to multiplied by β so as to ensure the correct energy dependence of the cross section.

The second-order calculation of Moroi *et al.*[12] of the single-quantum pair-annihilation cross section was used to correct the low-energy dependence by adding a term with a factor $(\alpha Z)^2$. The above procedure is implemented by multiplying the function f_{ME} by the first three terms of equation (2.34) (see Section 4.1 for details).

By the above procedure we were able to arrive at a formula that approximates the results of other workers[6, 8]. The formula we devised is

$$\sigma(W) = \frac{4\pi r_0^2 Z(Z\alpha)^4}{3\left(W^2-1\right)^{1/2}(W+1)^2} \frac{\beta\left(1-\exp\left(-\frac{2\pi\alpha Z}{\beta}\right)\right)}{\left(1+\frac{2\pi\alpha Z}{\beta}\right)}\left(3W^2+2W+4\right)$$
$$-\frac{W^2\log\left(W+\left(W^2-1\right)^{1/2}\right)}{(W+1)^4\left(W^2-1\right)^{1/2}}+\frac{(\alpha Z)^2 W^2}{(W+1)^7\left(W^2-1\right)^{1/2}}. \qquad (2.37)$$

Here W is the positron kinetic energy and the other symbols have their usual meanings. Equation (2.37) fits the cross sections for atomic numbers from Z = 47 to 90. However, for Z < 47, the formula breaks down, and gives negative cross sections for low energy.

For the low-energy regime, the ratio of the number of DQA photons to the number of SQA photons becomes large. This implies that SQA cross sections should decrease. As a matter of fact, the low-energy DQA cross section increases rapidly over that of SQA when the positron energy decreases. This is because for low positron energy, conservation energy and momentum favours DQA as opposed to SQA. It is important to note that the dominant process for annihilation in flight is DQA. The cross section for this process is given by[5]

$$\sigma(W) = \frac{Z\pi r_0^2}{(W^2-1)(W+1)}$$
$$\times\left[\left(W^2+4W+1\right)\log\left(W+\sqrt{\left(W^2-1\right)}\right) - (W+3)\sqrt{\left(W^2-1\right)}\right]. \quad (2.38)$$

2.7 ATOMIC-ELECTRON SCREENING EFFECT

We now consider atomic-electron screening effects. The discussion in this section follows closely that given by Tseng and Pratt[6]. Atomic-electron screening effects cause appreciable modifications of the total pair-annihilation cross sections for low energies in heavy elements (Z > 47). For low-Z elements, screening effects are always important.

Screening effects in single-quantum pair-annihilation have a simple origin which is also observed in atomic pair production and the atomic photoelectric effect. Tseng and Pratt[18] have shown that screening is a normalisation effect. They found that screening leads to a change in the normalisation and this change is greater in low-Z elements and much larger for higher shells. It is about 1 - 25% for the K shell and about 10 - 90% for the L shell over the range[6] Z = 2 - 100. For high-Z elements, the very low-energy continuum-state normalisations are also sensitive to screening, while at higher energies the continuum normalisation is unaffected.

It has been observed[6, 20] that at small distances, a screened continuum electron or positron wave function corresponding to shifted energy δE is closer in shape to a point Coulomb wave function than a screened wave function of the same energy. The shifted energy is given by $\delta E_{\pm} = \pm(\varepsilon_s - \varepsilon_c)$, where + is for a positron and - is for an electron, while the subscripts s and c are for screened- and point-Coulomb potentials respectively and ε is the binding energy of the bound state. Tseng and Pratt[6] have predicted a relationship between the screened- and the point-Coulomb SQA total cross sections[8] resulting in photons of the same energy. This relation is

$$\sigma_s(E_{+s}) = \Xi^2 \frac{p_{+c}^2}{p_{+s}^2} \sigma_c(E_{+c}), \tag{2.39}$$

where Ξ is the ratio of the screened- to the point-Coulomb bound state normalisations, σ_S is the screened cross section, σ_C is the point-Coulomb cross section, $E_{+S} = E_{+C} - (\varepsilon_S - \varepsilon_C)$, p_{+S} is the momentum associated with the energy E_{+S} and p_{+C} is the momentum associated with the energy E_{+C}.

Screening effects are not important for energies $E_+ > 1.5mc^2$ and $Z = 47 - 90$. For low positron energies and elements of $Z > 47$, the atomic-electron screening increases the K-shell SQA cross section, while for low-Z elements the atomic screening decreases the cross section[8, 18].

2.8 BINDING-ENERGY EFFECT

It is known from calculations of inner-shell ionisation cross sections by charged particles that the influence of the projectile on the initial state of the atom in the low-energy regime cannot be neglected. This is due to the binding effect. We believe that this effect contributes to the SQA cross section. To date, this effect has not been included in SQA cross-section calculations.

When a positron penetrates deeply into the K-shell of the target atom, it increases the binding energy of the K-shell electron. This leads to an increase of the K-shell SQA cross section. This effect was first estimated by Basbas, Brandt, and Laubert[14] for the K-shell electron in the perturbed-stationary-state approximation for heavy projectiles in inner-shell ionisation processes.

The binding-energy change leads to the target electrons being more tightly bound to the K shell during an encounter with positrons. This results from the fact that at low velocities the positrons must penetrate deep within the K shell to cause annihilation. The increased binding-energy increases the probability of annihilation. The binding energy change for the K-shell, δE_b, is derived[14] as a function of the reduced distance $y=|R|/a_{2k}$ between the target atom and the positron, where $a_{2k}=a_0/Z_{2k}$, a_0 is the Bohr radius, $Z_{2k}=Z-\zeta$, and ζ is the screening parameter which is a function of Z. The change in binding energy δE_b is given by first-order perturbation theory as[14, 42]

$$\delta E_b = \int \psi_k^*(\vec{r}) \frac{Z_1 \alpha}{|\vec{R} - \vec{r}|} \psi_k(\vec{r}) d\vec{r} . \tag{2.40}$$

Here $\psi_k(\mathbf{r})$ is the unperturbed non-relativistic hydrogenic K-shell wave function, $\mathbf{R}$ is the positron co-ordinate for a straight-line trajectory and $\mathbf{r}$ is the electron co-ordinate. After carrying out the integral we obtain[14]

$$\delta E_b = \frac{2 Z_{2k} \Re}{y} \left[1 - (1 + y)\exp(-2y)\right], \tag{2.41}$$

where $\Re$ is 13.6 eV.

The positron excites the K-shell electron while moving with velocity $v < v_{2k}$ where $v_{2k} = Z_{2k}v_0$ at a distance $|\mathbf{R}| = (b^2 + v^2t^2)^{1/2}$ and b is the impact parameter. In the present context, the same approximations as in inner-shell ionisation processes can be assumed. We therefore follow the method due to Basbas *et al.*[14]. According to this formulation, the binding-effect factor κ is given as

$$\kappa = 1 + \frac{2Z_1}{Z_{2k}\theta_k} g(\xi_k), \text{ where } Z_{2k} = Z_2 - 0.3,$$

$$\theta_k = \frac{|U|}{Z_{2k}^2 \Re}, \ \xi_k = \frac{2\eta_k^{1/2}}{\theta_k}, \eta_k = \frac{v_1^2}{Z_{2k}^2 v_0^2}, \text{ and } v_0 = \frac{e^2}{\hbar}.$$

The increased binding energy is given by[15] U' = κU. The difference $|U' - U| = \delta E_b$, is the binding-energy change. We note that U is the binding energy of the shell in question. The expression for $g(\xi_k)$ is

$$g(\xi_k) = (1 + \xi_k)^{-5}\left(1 + 5\xi_k + 7.14\xi_k^2 + 4.27\xi_k^3 + 0.947\xi_k^4\right). \qquad (2.42)$$

At high positron energies, $\xi_k >> 1$, and the binding effect vanishes. When $\xi_k << 1$, the binding effect, although due only to a small perturbation[14] $(\kappa - 1) \le 2Z_1/Z_{2k}\,\theta_k$, can become large. Z_1 is the charge of the projectile; in this case since the projectile is a positron, it is unity.

For an exact calculation, we use the unperturbed relativistic hydrogenic wave functions in equation (2.40a). In this case the change in binding energy is given by[42]

$$\delta E_b = Z_1\alpha\left[\int_0^R \frac{r^2\left(g_\kappa^2 + f_\kappa^2\right)dr}{R} + \int_R^\infty r\left(g_\kappa^2 + f_\kappa^2\right)dr\right] \qquad (2.43)$$

where $R = |\mathbf{R}|$, $r = |\mathbf{r}|$, g and f are the radial functions (equation 2.4) of the K shell electron. We have however used the non-relativistic case (equation 2.40) to simplify our calculation.

We note that our calculation of the binding factor is approximate. This is because in the case of high-Z targets, it is necessary to use relativistic wave functions for target electrons, as the relativistic wave functions for heavy elements are considerably different from their non-relativistic ones[42].

By use of the method of Section 2.7, it is possible to incorporate the binding-energy change effect into the point-Coulomb cross sections[21]. In the equation $E_{+s} = E_{+c} - (\varepsilon_s - \varepsilon_c)$, where E_+ is the positron energy, we add the binding-energy change δE_b. The new positron energy is then defined as

$$E'_{+s} = E_{+c} - (\delta E_{TP} + \delta E_b), \tag{2.44}$$

where $\delta E_{TP} = \varepsilon_s - \varepsilon_c$ and $\delta E_b = |U|(\kappa - 1)$.

We have adopted the method of Tseng and Pratt[6] because it connects the screened cross sections and the point-Coulomb cross sections in a simple manner. Otherwise an exact calculation of the relationship between screened and point-Coulomb cross sections has been performed by Broda and Johnson[8].

CHAPTER 3

THE SQA CROSS SECTION AND THE CALCULATION OF PHOTON MASS ENERGY-ABSORPTION COEFFICIENTS

3.1 ATTENUATION COEFFICIENT

Consider a slab of material of thickness t, which is irradiated with a narrow beam of electromagnetic radiation. The radiation passing through is attenuated according to

$$I(t) = I_0 \exp(-\mu t), \tag{3.1}$$

where I_0 is the intensity of electromagnetic radiation incident on the material and μ is the total linear attenuation coefficient. In situations more complex than the narrow beam, the attenuation is still exponential but is modified by two additional factors[35]. The first of these is the 'geometry factor'. This depends essentially on the source geometry and includes, for example, the insertion of the inverse square law in equation (3.1) for a point isotropic source. The other factor, often called the 'build-up factor', takes into account secondary photons produced in the absorber which reach the detector[35].

From the above, it is apparent that the linear attenuation coefficient μ is proportional to the density ρ of the absorber, which usually does not have a *unique value but depends to some extent on the physical state of the material.*

To remove this density dependence we use the mass attenuation coefficient μ/ρ, which has units of area/mass.

The mass attenuation coefficient is defined as[13]

$$\frac{\mu}{\rho}(T) = \frac{N_a}{A}\sum_j \sigma_j(T) = \frac{N_a}{A}\sigma_{tot}(T), \tag{3.2}$$

where N_a is Avogadro's number and A is the relative atomic mass of the target element. Equation (3.2) is written to indicate that the total cross section (and the attenuation coefficient) is the sum of partial cross sections (and the component attenuation coefficients) for interactions of the j type.

The total cross section σ_{tot} is written as a sum over contributions from principal photon interactions[35]

$$\sigma_{tot} = \sigma_{coh} + \sigma_{incoh} + \tau + \kappa + \sigma_{ph.n}, \tag{3.3}$$

where σ_{coh} and σ_{incoh} are coherent (Rayleigh) and incoherent (Compton) scattering cross sections respectively; τ is the atomic-photoeffect cross section; κ is the positron-electron pair production (including triplet) cross section; and $\sigma_{ph.n}$ is the photonuclear cross section.

3.2 MASS ENERGY-ABSORPTION COEFFICIENT

The mass energy-absorption coefficient is related to the mass attenuation coefficient by the formula[13]

$$\frac{\mu_{en}}{\rho} = \frac{N_a}{A}\sum_j f_j\left(1 - G_j\right)\sigma_j$$
$$\frac{\mu_{en}}{\rho} = f(1 - G)\frac{\mu}{\rho} \tag{3.4}$$

where[13] G_j is the average fraction of the kinetic energy of secondary charged particles produced in an interaction of type j that is subsequently lost in radiative processes, and G is the weighted average of G_j. f_j is the average fraction of the photon energy that is transferred to kinetic energy of charged particles in interaction of type j, and f is the weighted average of f_j.

G_{pair} is the fraction of energy that corresponds to positron-electron pair and triplet processes. This includes kinetic energy transferred to photons by in-flight positron annihilation[38]. The mass energy-absorption coefficient for pair production has two radiative loss components. One is the bremsstrahlung component for electrons and positrons and the other is the in-flight positron annihilation component. These two components are folded into a single correction factor for G_{pair} and the contribution to the mass energy-absorption is written as $\sigma_{pair}/\rho(1 - G_{pair})f_{pair}$. G_{pair} includes a contribution from SQA through the annihilation flight factor. Positron-electron pairs created are subsequently annihilated with the emission of one or two photons[40].

3.3 ANNIHILATION FLIGHT FACTOR

The probability that a positron of initial energy T_0 (MeV) annihilates when it slows down to an energy between T and dT is given by[13]

$$W(T,T_0)dT = \exp\left\{-\int_T^{T_0}\omega_a(T')dT'\right\}\omega_a(T)dT \quad (3.5)$$

where ω_a is the probability of annihilation per unit energy interval. This quantity is obtained from the cross section per atom for annihilation in flight, σ_a, in the continuous-slowing-down approximation and is given by[13]

$$\omega_a(T) = \frac{N_a\sigma_a(T)}{AS_{tot}(T)}, \quad (3.6)$$

where S_{tot} is the stopping power for the positron in the medium as a whole, A is the atomic mass and N_a is Avogadro's number. The dominant process for annihilation in flight is the two-quantum annihilation (DQA) given by equation (2.38). The SQA contribution to the probability of annihilation per energy interval $\omega_a(T)$, is through the cross section. In equation (3.7) for $\omega_a(T)$ the cross section σ_a is defined as $\sigma_a = \sigma_{2a} + \sigma_{1a}$, where σ_{2a} is the DQA cross section and σ_{1a} is the SQA K-shell cross section.

The total stopping power S_{tot} is expressed as a sum[5] of the mass radiative stopping power and the mass collision stopping power. The mass collision stopping power is due to energy transfer from the incident particle to the bound atomic electrons. The mass collision stopping power[23] can be expressed as

$$S_{col}(T) = \frac{2\pi N_a r_0^2 mc^2}{\beta^2}\frac{Z}{A}\left[\log\left(\frac{T}{I}\right)^2 + \log\left(1+\frac{\tau}{2}\right) + F^+(\tau) - \delta\right] \quad (3.7)$$

where $\tau = T/mc^2$, the kinetic energy of the incident positron in units of the electron rest mass, N_aZ/A represents the number of atomic electrons per gram of the medium, $N_a = 6.022045 \times 10^{23}\ mol^{-1}$, which is Avogadro's number, I is the mean ionisation energy, and Z and A are the atomic number and atomic mass respectively. The function $F^{+}(\tau)$ is

$$F^{+}(\tau) = 2\log(2) - \left(\frac{\beta^2}{12}\right)\left[23 + \frac{14}{(\tau+2)} + \frac{10}{(\tau+2)^2} + \frac{4}{(\tau+2)^3}\right] \tag{3.8}$$

and δ is the density-effect correction, which can be ignored for most calculations. For electron-electron interactions F^{+} is different from the form given above.

The mass radiative stopping power is expressed in terms of the bremsstrahlung cross section as[23]

$$S_{rad}(T) = \frac{N_a}{A}\left[\int_0^T k\frac{d\sigma_n}{dk}dk + Z\int_0^{T'} k\frac{d\sigma_e}{dk}dk\right], \tag{3.9}$$

where $d\sigma_n/dk$ is the differential cross section for the emission of a photon of energy k due to the interaction of the positron with the screened Coulomb field of the atomic nucleus, and $d\sigma_e/dk$ is the corresponding cross section for the Coulomb interaction with one of the atomic electrons. The upper limit T' is given as $T'=mc^2T[T + 2mc^2 - \beta(T + mc^2)]^{-1}$. It is convenient[23] to introduce the functions

$$\Phi_{rad}^{(n)} = (\alpha r_0^2 Z^2)^{-1}\int_0^T \left(\frac{k}{E}\right)\frac{d\sigma_n}{dk}dk$$

and

$$\Phi_{rad}^{(e)} = (\alpha r_0^2)^{-1}\int_0^{T'} \left(\frac{k}{E}\right)\frac{d\sigma_e}{dk}dk \tag{3.10}$$

where $E = T + mc^2$ is the total energy of the positron. In terms of these *quantities the mass radiative stopping power can be written as*

$$S_{rad}(T) = \frac{N_a}{A}\alpha r_0^2 E Z^2 \Phi_{rad}^{(n)}(T)\left[1 + \frac{1}{Z}\frac{\Phi_{rad}^{(e)}(T)}{\Phi_{rad}^{(n)}(T)}\right] \tag{3.11}$$

where $\Phi_{rad}^{(e)}(T)/\Phi_{rad}^{(n)}(T)$ is approximately unity at high energies and vanishes at low energy. The differential cross section for the emission of a photon in the high-energy limit is given as[23]

$$k\frac{d\sigma_n}{dk} = 4\alpha r_0^2 Z^2 \sum_{i=1}^{2} g(E,k)\left[e_i + \int_{q_0}^{1} h_i(q)\{1-F(q,Z)\}^2 - f(Z)\right] \tag{3.12}$$

where q is the momentum transfer and $q_0 = mc^2k/[2E(E-k)]$, the minimum momentum transfer (in mc units). The Coulomb correction is given as[23]

$$f(Z) = (\alpha Z)^2 \sum_{n=1}^{\infty} \frac{1}{n\left(n^2 + (\alpha Z)^2\right)}. \tag{3.13}$$

The other differential cross section $k\frac{d\sigma_e}{dk}$ is similar to $k\frac{d\sigma_n}{dk}$ except that f(Z) is set equal to zero, $[1 - F(q,Z)]^2$ is replaced by S(q,Z) and Z outside the summation is set equal to one. S(q,Z) is normalised such that[23, 43] $S(\infty,Z) = 1$. In the literature, this function S(q,Z) is known as the incoherent scattering function. The other quantities are defined[23] as follows:

$$g_1 = 1 + \left(\frac{E-k}{E}\right)^2,\ g_2 = \frac{2(E-k)}{3E},\ e_1 = 1,\ e_2 = 5/6$$
$$h_1 = \frac{(q-q_0)^2}{q^3},\ h_2 = \frac{\left[q^3 - 6q_0^2 q\log\left(\frac{q}{q_0}\right) + 3q_0^2 q - 4q_0^3\right]}{q^4}. \tag{3.14}$$

In these expressions, F(q,Z) is the atomic form factor normalised such that F(0,Z) = 1. Hubbell *et al.*[24] have given the atomic form factor, which incorporates electron-correlation effects, for a pure Coulomb potential $V(r) = -(\alpha Z)/r$ as

$$F(q,Z) = \frac{(2Z\alpha)^{2\gamma+1}}{\gamma q} \frac{\sin\left[2\gamma \arctan\left(\frac{q}{2Z\alpha}\right)\right]}{\left[(2Z\alpha)^2 + q^2\right]^{\gamma}}, \tag{3.15}$$

with $\gamma = (1 - (\alpha Z)^2)^{1/2}$. The square of the atomic form factor is the probability that the Z electrons of an atom take up a recoil momentum q without absorbing any energy.

The theory presented above is only approximate at low energy, being more valid for high energy. This is because electrons are attracted by the nuclear charge and are repelled by the orbital electrons; the opposite behaviour prevails for positrons. This leads to differences between the bremsstrahlung cross section for electrons and positrons. However, these differences are small at high energies.

At low energies, the bremsstrahlung cross section for positrons is considerably smaller than that for electrons of the same energy[25, 26]. Finally the total stopping power is expressed as $S_{tot} = S_{rad} + S_{col}$. Now, the probability of annihilation at rest is[13]

$$W_0(T_0) = 1 - \int_0^{T_0} W(T,T_0)dT = \exp\left\{-\int_0^{T_0} \omega_a(T)dT\right\}. \tag{3.16}$$

The kinetic energy not radiated away in the course of slowing down is then

$$\begin{aligned} D(T_0) = T_0 - \{W_0(T_0)T_0Y(T_0) + \int_0^{T_0} W(T,T_0)[T_0Y(T_0) - TY(T)]dT \\ + \int_0^{T_0} W(T,T_0)TdT\}, \end{aligned} \tag{3.17}$$

where in the curly brackets, the first term is the average radiative loss for those positrons slowing down to rest, the second term is the average radiative loss for the positrons in the course of slowing down, and the third term is the average of the positron's kinetic energy at the time of annihilation in flight. Rearranging the terms we have[13]

$$D(T_0) = T_0\,\{1-Y(T_0)-\eta(T_0)\}, \tag{3.18}$$

where

$$\eta(T_0) = \frac{1}{T_0}\int_0^{T_0} W(T,T_0)T[1-Y(T)]dT, \tag{3.19}$$

and Y(T) is the total radiative yield. The radiative yield (also called the bremsstrahlung efficiency) is the fraction of the initial kinetic energy T_0 of a positron that is converted to bremsstrahlung energy as the positron slows down to rest. The continuous-slowing-down approximation yield is given[13, 23] by

$$Y(T_0) = \frac{1}{T_0}\int_0^{T_0} \frac{S_{rad}(T)dT}{(S_{col}(T)+S_{rad}(T))}. \tag{3.20}$$

The factor $\eta(T_0)$ in equation (3.19) is known as[13] the annihilation flight factor.

3.4 ABSORPTION COEFFICIENT AND THE ANNIHILATION FLIGHT FACTOR

Equation (3.19) is related to the photon mass energy-absorption coefficient[13]. From equation (3.4) the mass energy-absorption coefficient is defined in terms of G and it is related to the attenuation coefficient μ/ρ. The G_{pair}

corresponding to pair and triplet production also includes in-flight positron annihilation[13, 38]. G_{pair} is related to the annihilation flight factor η through[13]

$$
\begin{aligned}
G_{pair} = \frac{1}{\left[f_{pair} E\mu_{pair}(E)\right]} \int_{0}^{E-2mc^2} & \left[\sum_{i} w_i \mu_{pair,\,i}(E) P_{pair,\,i}(T_+)\right] \\
& \times \left\{\left(E - 2mc^2 - T_+\right) Y_-\left(E - 2mc^2 - T_+\right) + T_+\left[Y_+(T_+) + \eta(T_+)\right]\right\} dT_+ ,
\end{aligned}
\tag{3.21}
$$

where the kinetic energy of the electron is $T_- = E - 2mc^2 - T_+$, w_i is the fraction by weight of the ith atomic constituent, E is the photon energy in MeV and $P_{pair,}(T_+)$ is the probability that a positron from pair production will have kinetic energy between T_+ and $T_+ + dT_+$ and is defined as

$$
P_{pair}(T_+) dT_+ = \frac{d\sigma_{pair}(W)}{dW} dT_+ \Bigg/ \int_{1}^{k-1} \frac{d\sigma_{pair}(W)}{dW} dW , \tag{3.22}
$$

where k is the photon energy in units of electron rest mass and W is the total energy of the positron in units of electron rest mass. μ_{pair} is the linear attenuation coefficient corresponding to pair production. Y(T) in equation (3.21) is the radiative yield, with the + corresponding to the positron and the - to the electron.

Equations (3.4) and (3.21) establish a relationship between the annihilation flight factor η and the photon mass energy-absorption coefficient. Therefore, SQA contributes to the calculation of the mass energy-absorption coefficient through the annihilation flight factor. We did not calculate the photon mass energy-absorption coefficient since this would have taken us beyond the level and scope of this thesis.

CHAPTER 4

RESULTS

4.1 THE SQA CROSS SECTION

In this section we discuss the results from the formula we have devised (equation (2.37)) in relation to the results due to Tseng and Pratt[6] and to Broda and Johnson[8] and to the Born approximation result, equation (2.34).

In the derivation of equation (2.37), the modified Elwert factor (equation (2.36)), is multiplied by the first three terms of equation (2.34). The motivation for multiplying by this factor comes from Seltzer's[13] result in which a factor similar to the modified Elwert factor appears, though with a negative instead of a positive sign in the denominator.

The exact numerical results due to Tseng and Pratt[6] and to Broda and Johnson[8] were used to approximate an analytical K-shell SQA cross section formula (see equation (2.37)). Figures 4.1, 4.2, 4.3 and 4.4 are the result of this approximate formula. Comparison plots from references 6 and 8 and that of the Born approximation, equation (2.34) are plotted in the same figures as above. The cross sections are in barns (10^{-28} m^2).

We note that the agreement for high-Z values ($Z > 70$) with the exact results[6, 8] is better than that of the results due to Seltzer[13] (see Figures 4.10 and 4.11). We have tabulated some values obtained from equation (2.37) in

Table 4.1, for Z = 47, 74, 82 and 90. The computer code that was used to obtain these results is given in the appendix (see App.1).

4.2 BINDING-ENERGY EFFECT ON SQA CROSS SECTION

This section gives results of our calculation of the binding-energy effect on the SQA cross section.

The binding-energy effect on the SQA cross section is illustrated in the plots of Figures 4.5, 4.6, 4.7, and 4.8, for the same atomic numbers as in Section 4.1. The resulting cross sections are given in Table 4.2. The cross sections are higher than those due to the screened potential[6, 8] and those obtained by use of the point-Coulomb potential[21]. Since the difference with the other two results (Tseng and Pratt[6] and Broda and Johnson[8]) is more pronounced at low energy, it indicates that the binding-energy effect cannot be ignored in the low-energy region.

The results due to Tseng and Pratt[6] were reproduced by use of equation (2.39). The point-Coulomb cross sections (σ_c in equation (2.39)) were taken from Johnson *et al.*[21]. The results from this computer code (see App.3) are in good agreement with the original results in reference 6. The major differences are at low energies, where Tseng and Pratt 's[6] results are higher than those obtained from our computer code.

For instance, at positron energy 1.0625mc^2 and Z = 47, our FORTRAN program (excluding the binding-energy effect) gives a cross section value of

0.0140 barns while Tseng and Pratt[6] give 0.0176. These differences are noticed for all elements. Almost perfect agreement occurs at energies higher than $1.1875mc^2$, where the error is less than 0.01%.

We incorporate the binding-energy effect into the point-Coulomb SQA cross sections by use of a method due to Tseng and Pratt[6]. We have modified the equation they use, though all contributions from screening effect are still taken into consideration. The screened positron energy is now written such that the binding-energy change and the screening effects are included. Thus the screened positron energy is written as $E'_{+s} = E_{+c} - (\delta E_{TP} + \delta E_b)$ and Equation (2.39) now becomes

$$\sigma_s\left(E'_{+s}\right) = \Xi^2 \frac{p^2_{+c}}{p'^2_{+s}} \sigma_c\left(E_{+c}\right), \tag{4.1}$$

where E_{+c} is the positron energy, $p^2_{+c} = E^2_{+c} - 1$ and $p'^2_{+s} = E'^2_{+s} - 1$. Ξ is defined as[6]

$$\Xi = \lim_{r\to 0} \frac{G^s_K(r)}{G^c_K(r)} = \lim_{r\to 0} \frac{F^s_K(r)}{F^c_K(r)}, \tag{4.2}$$

which is the ratio of screened (s) to point-Coulomb bound-state(c) normalisations for a given state K. In equation (4.2) G and F are the bound-state wave functions with normalisation. $\sigma_c(E_{+c})$ is the SQA K-shell cross section of Johnson *et al.*[21] and $\sigma_s(E'_{+s})$ is the SQA K-shell cross section which now includes the screening effect and the binding-energy effect. In all the above calculations energies are in units of mc^2.

A FORTRAN program (see Appendix, App.3) was written to evaluate equation (4.1). The values of Ξ are those given by Tseng and Pratt[6]. We have tabulated the values of δE_b (see equation 2.44) and the binding factor κ for $Z = 47$ to 90 in Table 4.3 and we have given the cross sections resulting from this calculation in Table 4.2.

Table 4.1: SQA cross section as a function of energy for various Z values. These values correspond to our closed formula, equation (2.37).

Energy (mc^2)	Z = 47	Z = 74	Z = 82	Z = 90
1.0625	0.0121	0.2993	0.4854	0.7360
1.1250	0.0205	0.3819	0.6126	0.9240
1.1875	0.0266	0.4217	0.6736	1.0142
1.2500	0.0312	0.4417	0.7039	1.0589
1.3125	0.0346	0.4510	0.7176	1.0788
1.3750	0.0372	0.4539	0.7214	1.0839
1.4375	0.0391	0.4529	0.7191	1.0800
1.5000	0.0405	0.4495	0.7130	1.0704
1.5625	0.0415	0.4445	0.7045	1.0419
1.6250	0.0423	0.4385	0.6945	1.0253
1.6875	0.0428	0.4320	0.6837	1.0079
1.7500	0.0431	0.4251	0.6723	0.9726
1.8750	0.0433	0.4111	0.6492	0.9379
2.0000	0.0432	0.3971	0.6265	0.9379
2.2500	0.0421	0.3711	0.5841	0.8733
2.5000	0.0406	0.3480	0.5465	0.8161
2.7500	0.0390	0.3276	0.5135	0.7659
3.0000	0.0374	0.3096	0.4843	0.7216
3.2500	0.0358	0.2936	0.4585	0.6825
3.5000	0.0342	0.2792	0.4354	0.6476

Table 4.2: SQA cross sections as a function of energy for various Z values. These cross sections include screening and binding energy effects on point-Coulomb[21] results.

Energy(mc^2)	Z=47	Z=74	Z=82	Z=90
1.0625	0.0141	0.0317	0.0334	0.0344
1.1250	0.0330	0.1583	0.2049	0.2494
1.1875	0.0429	0.2841	0.4053	0.5440
1.2500	0.0474	0.3710	0.5599	0.7974
1.3125	0.0492	0.4223	0.6624	0.9773
1.3750	0.0495	0.4488	0.7140	1.0923
1.4375	0.0492	0.4594	0.7508	1.1580
1.5000	0.0485	0.4603	0.7593	1.1870
1.5625	0.0478	0.4534	0.7552	1.1924
1.6250	0.0468	0.4441	0.7427	1.1815
1.6875	0.0459	0.4320	0.7257	1.1592
1.7500	0.0451	0.4192	0.7052	1.1308
1.8750	0.0435	0.3933	0.6626	1.0661
2.0000	0.0421	0.3682	0.6192	0.9977
2.2500	0.0397	0.3272	0.5452	0.8751
2.5000	0.0377	0.2954	0.4864	0.7746
2.7500	0.0359	0.2691	0.4399	0.6946
3.0000	0.0343	0.2482	0.4010	0.6301
3.2500	0.0326	0.2305	0.3697	0.5755
3.5000	0.0311	0.2140	0.3417	0.5295

Table 4.3: Values of δE_{TP}, δE_b, Ξ, and κ.

Z	δE_{TP} (mc^2)	δE_b (mc^2)	Ξ^2	κ
47	0.0108	4.285E-04	0.9801	1.0071
73	0.0214	1.016E-03	0.9852	1.0067
74	0.0219	1.044E-03	0.9853	1.0066
78	0.0240	1.159E-03	0.9858	1.0065
79	0.0244	1.189E-03	0.9859	1.0065
82	0.0259	1.281E-03	0.9861	1.0065
90	0.0310	1.545E-03	0.9867	1.0063

Note: Ξ and δE_{TP} are those given by Tseng and Pratt[6], κ is the binding factor corresponding to energy $1.125mc^2$ and δE_b is the binding energy change at $2.5mc^2$.

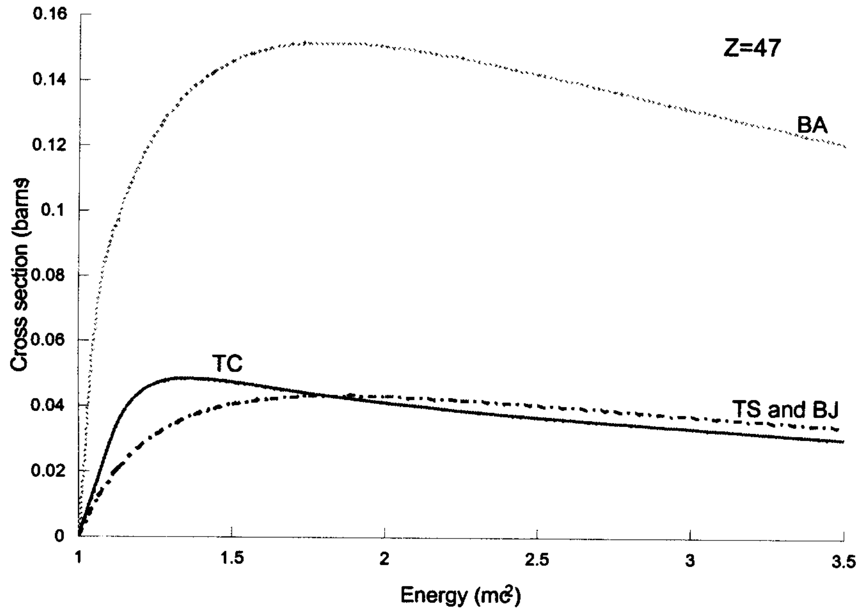

Figure 4.1. A plot of the Born approximation (BA), this calculation (TC), the result due to Tseng and Pratt[6] (TS), and to Broda and Johnson[8] (BJ)

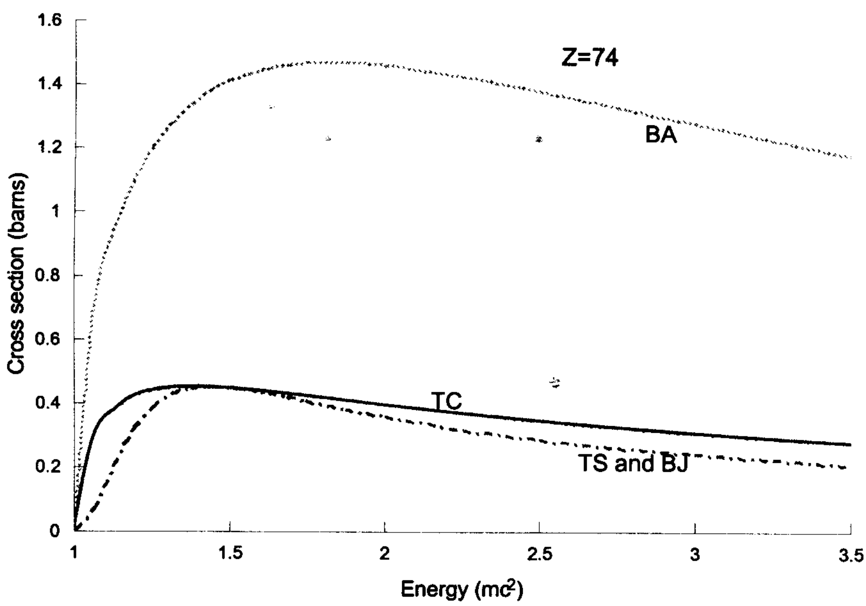

Figure 4.2. A plot of the Born approximation (BA), this calculation (TC), the result due to Tseng and Pratt[6] (TS), and to Broda and Johnson[8] (BJ)

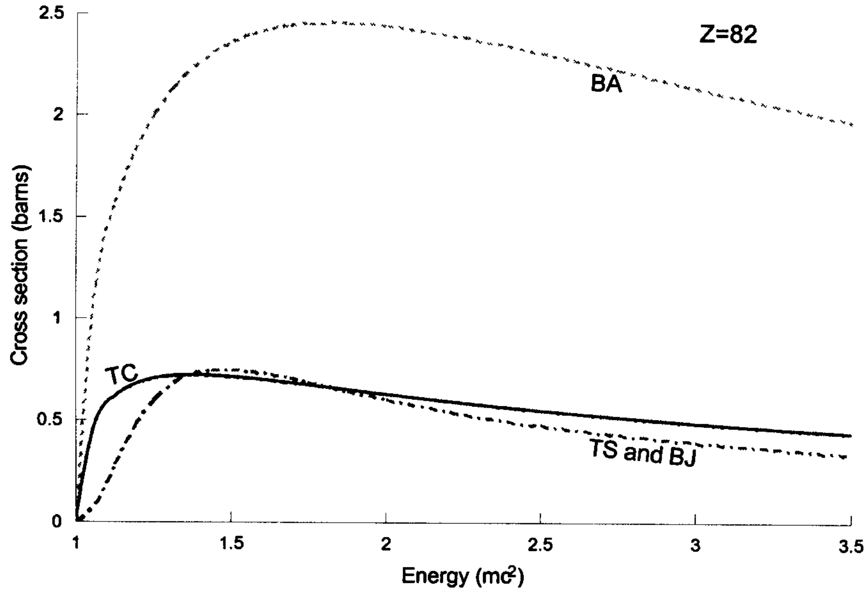

Figure 4.3. A plot of the Born approximation (BA), this calculation (TC), the result due to Tseng and Pratt[6] (TS), and to Broda and Johnson[8] (BJ).

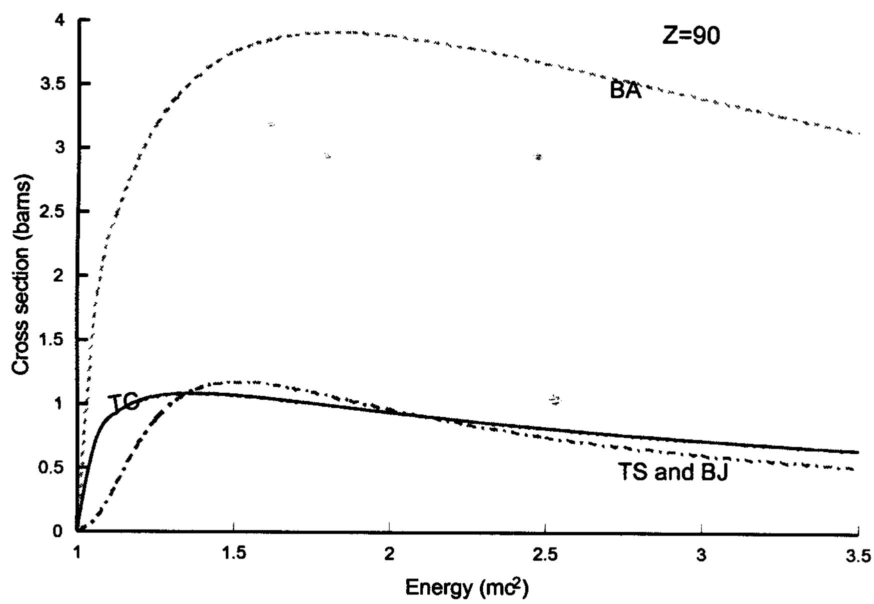

Figure 4.4. A plot of the Born approximation (BA), this calculation (TC), the result due to Tseng and Pratt[6] (TS), and to Broda and Johnson[8] (BJ).

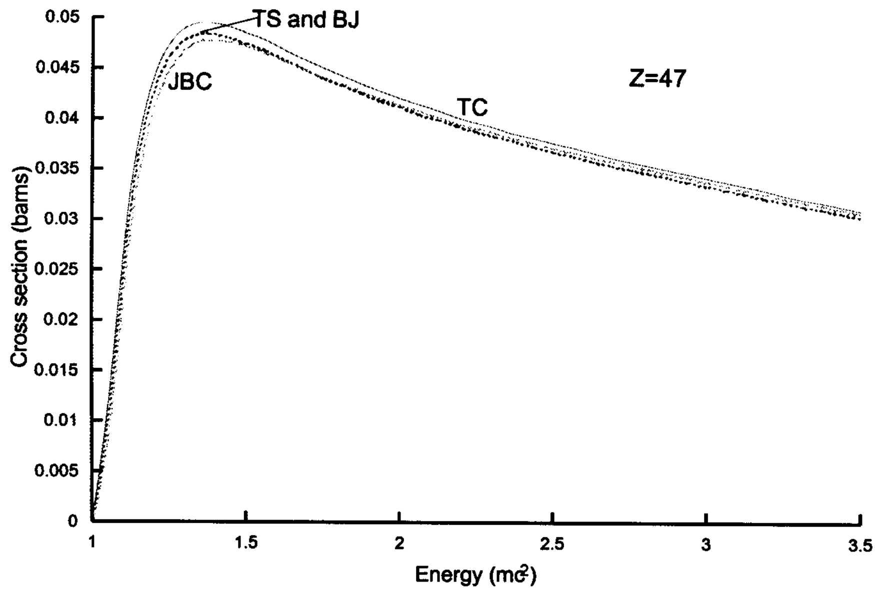

Figure 4.5. A plot of the K shell cross section due to binding energy effect (TC), and the original Johnson *et al.*[21] (JBC) cross sections, including the result due to Tseng and Pratt[6] (TS), and to Broda and Johnson[8] (BJ).

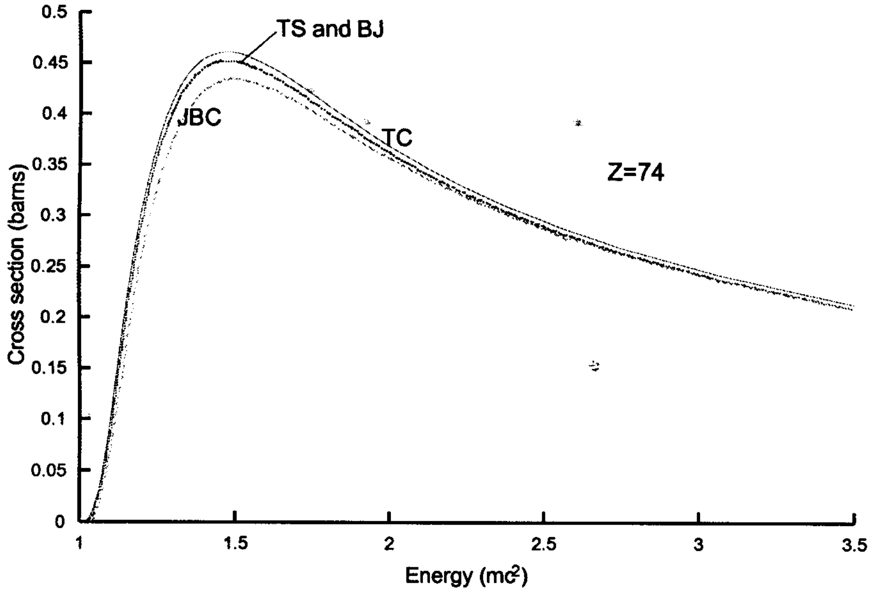

Figure 4.6. A plot of the K shell cross section due to binding energy effect (TC), and the original Johnson *et al.*[21] (JBC) cross sections, including the result due to Tseng and Pratt[6] (TS), and to Broda and Johnson[8] (BJ).

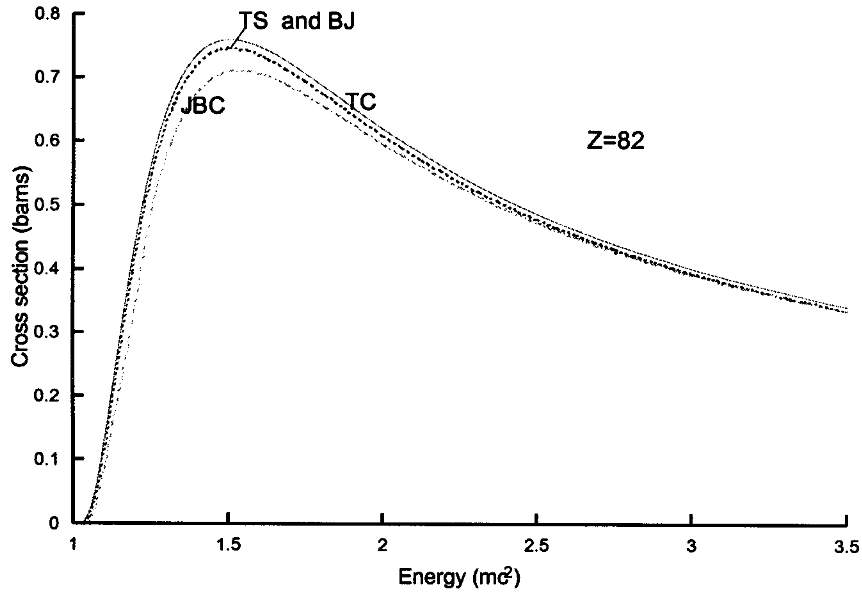

Figure 4.7. A plot of the K shell cross section due to binding energy effect (TC), and the original Johnson *et al.*[21] (JBC) cross sections, including results due to Tseng and Pratt[6] (TS), and to Broda and Johnson[8] (BJ).

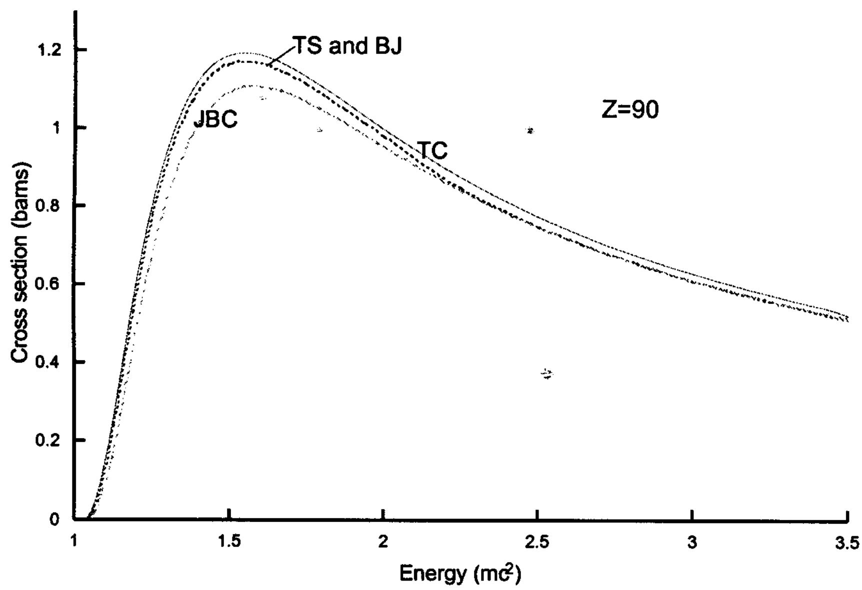

Figures 4.8. A plot of the K shell cross section due to binding energy effect (TC), and the original Johnson *et al.*[21] (JBC) cross sections, including results due to Tseng and Pratt[6] (TS), and to Broda and Johnson[8] (BJ).

4.3 COMPARISON OF SQA MODELS

In this section, we compare the results from our new formula equation (2.37) with those from Seltzer's[13] analytical formula (equation (2.33) and the SQA screened results of Broda and Johnson[8] and those of Tseng and Pratt[6]. The comparison is done for Z = 47, 82, and 90. The various results are plotted in Figures 4.9, 4.10 and 4.11 respectively.

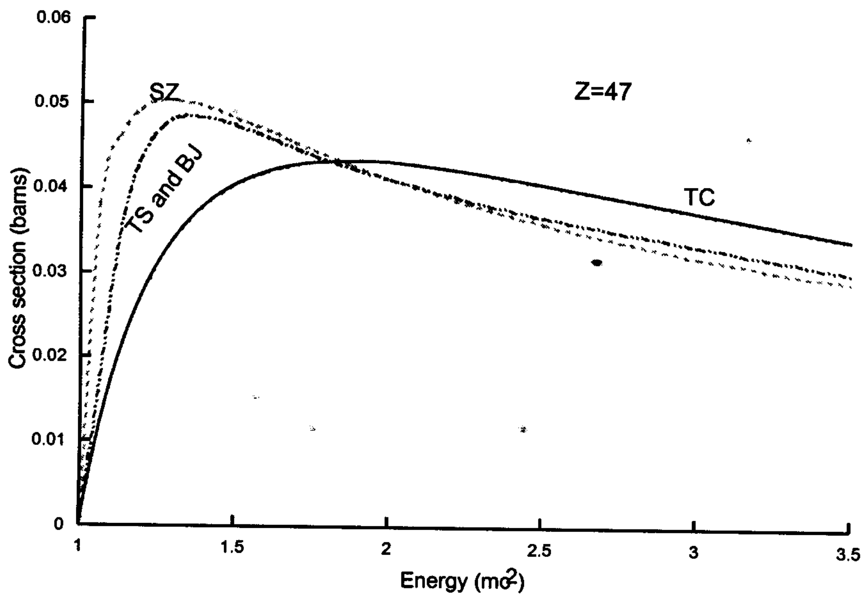

Figure 4.9 Comparison of SQA models, Seltzer's[13] result (SZ), Tseng and Pratt[6] (TS) results and Broda and Johnson[8] (BJ) results and this calculation (TC).

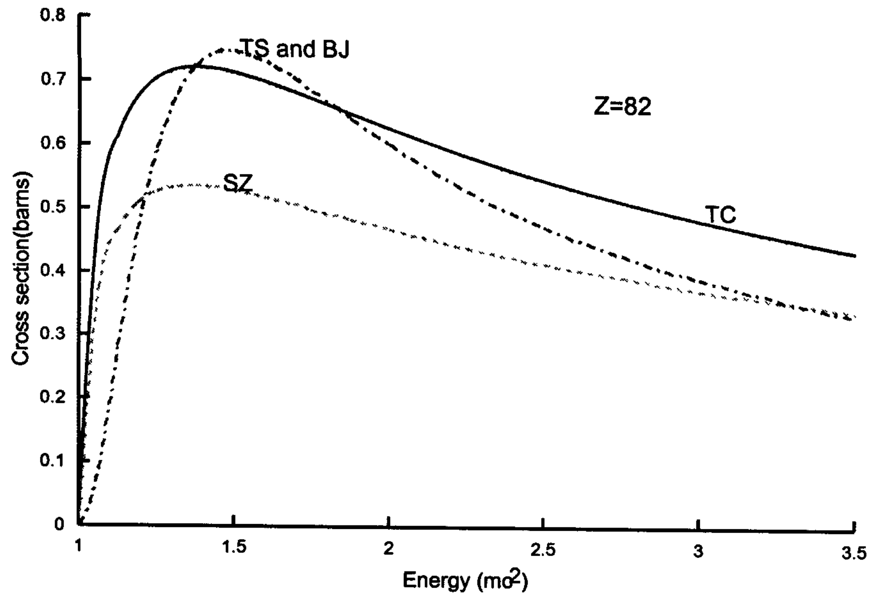

Figure 4.10 Comparison of SQA models, Seltzer's[13] result (SZ), Tseng and Pratt[6] (TS) results and Broda and Johnson[8] (BJ) results and this calculation (TC).

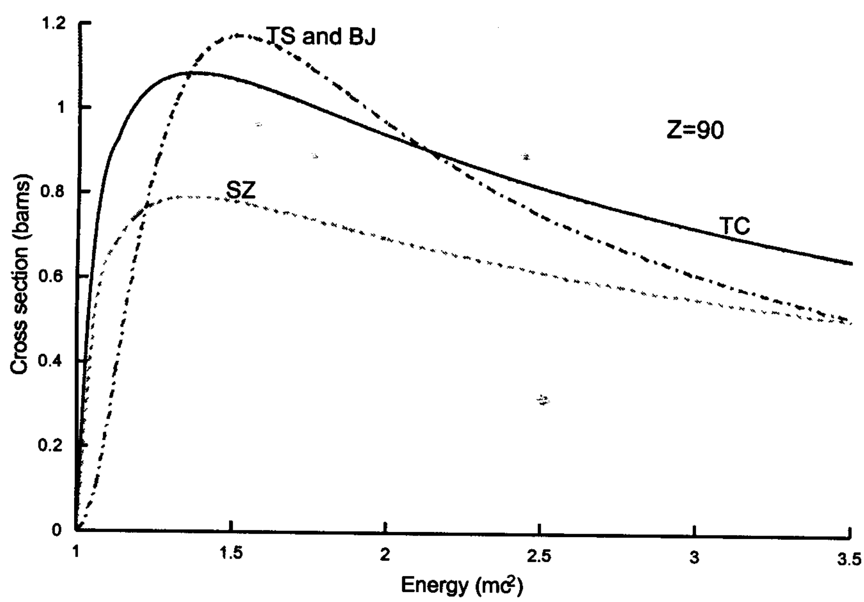

Figure 4.11 Comparison of SQA models, Seltzer's[13] result (SZ), Tseng and Pratt[6] (TS) results and Broda and Johnson[8] (BJ) results and this calculation (TC).

We note that from Figure 4.9 ($Z = 47$) that our approximate formula (equation (2.38)) yields a plot of poor shape compared to Seltzer's[13] result and the exact results from references 6 and 8. However, though the approximation is not very good, the correct energy dependence of the SQA cross section is still reproduced.

Our SQA cross-section formula approximates well the exact cross sections of references 6 and 8 for high-Z values. Therefore our formula is in good agreement with the theory of SQA, according to which SQA cross section increases with increasing Z-value. This can be seen in Figures 4.10 and 4.11, for $Z = 82$ and 90 respectively. From these figures, we note that our result is a better approximation than that of Seltzer[13], which is about half the exact value.

The maxima of the plots for high-Z values are shifted to the low-energy region; this is an indication that our approximate formula gives slightly higher cross-section values at low energy as compared to those of references 6 and 8. For low-Z values, the maximum is flat and shifted toward the high-energy end. This indicates that our formula gives low cross sections for low-Z values and at low energy. At high energy our results are higher than those of other workers[6, 8].

4.4 Z-DEPENDENCE OF SQA CROSS SECTION

Using the cross sections that include screening effects and binding-energy effects (Section 2.8) and for the energies between 1.0625 to 1.1875mc^2 from Table 4.2, graphs of $\log(\sigma)$ versus $\log(Z)$ were plotted in an attempt to determine a simple Z-dependence for the total SQA cross section for an atom. Following Sheth and Swamy[10], the dependence was assumed to be of the form

$$\sigma \sim Z^{n}. \tag{4.3}$$

The slopes of the curves were found to vary much with energy. The average value of n was found to be approximately 4.03. This result compares well with earlier calculations which yielded n ~ 4.4 (in reference 10).

We note in passing that recent experiments[22] have reported a value for n of approximately 5.1. Bergstorm *et al.*[27] discuss in detail these discrepancies between experiment and theory.

4.5 NUMERICAL DETAILS: ANNIHILATION FLIGHT FACTOR

In the numerical evaluation of equation (3.19), we did not use explicit expressions for $S_{tot}(T)$ and $Y(T)$; rather, interpolation was used. This is because we did not have analytical expressions for these quantities. For instance, neither $S_{rad}(T)$ nor $S_{col}(T)$ is known accurately below an intermediate energy[23] T_i = 1keV. Therefore, interpolation and extrapolation were used to obtain values of $S_{rad}(T)$ and $S_{col}(T)$ between tabulated ones.

The interpolation routine used employed rational functions[19]. The reason for this choice was that rational functions have the ability to model functions with poles. The expression for $Y(T)$, equation (3.20), is a ratio of $S_{rad}(T)$ and $S_{tot}(T)$. This ratio might have poles for certain values of energy T. The values of $S_{tot}(T)$ and $Y(T)$ taken from reference 23 were interpolated in order to perform the determine a simple Z-dependence for the total SQA cross section for an atom. Following Sheth and Swamy[10], the dependence was assumed to be of the form

$$\sigma \sim Z^n . \tag{4.3}$$

The slopes of the curves were found to vary much with energy. The average value of n was found to be approximately 4.03. This result compares well with earlier calculations which yielded n ~ 4.4 (in reference 10).

We note in passing that recent experiments[22] have reported a value for n of approximately 5.1. Bergstorm *et al.*[27] discuss in detail these discrepancies between experiment and theory.

4.5 NUMERICAL DETAILS: ANNIHILATION FLIGHT FACTOR

In the numerical evaluation of equation (3.19), we did not use explicit expressions for $S_{tot}(T)$ and $Y(T)$; rather, interpolation was used. This is because we did not have analytical expressions for these quantities. For instance, neither $S_{rad}(T)$ nor $S_{col}(T)$ is known accurately below an intermediate energy[23] T_i = 1keV. Therefore, interpolation and extrapolation were used to obtain values of $S_{rad}(T)$ and $S_{col}(T)$ between tabulated ones.

The interpolation routine used employed rational functions[19]. The reason for this choice was that rational functions have the ability to model functions with poles. The expression for $Y(T)$, equation (3.20), is a ratio of $S_{rad}(T)$ and $S_{tot}(T)$. This ratio might have poles for certain values of energy T. The values of $S_{tot}(T)$ and $Y(T)$ taken from reference 23 were interpolated in order to perform the

The contribution of SQA to the annihilation flight factor according to our formula equation (2.37), is seen in column seven of Table 4.3. It is about 3.5% on average for this calculation. The FORTRAN program used in these calculations is given in the Appendix (see App.2).

Table 4.3: Values of the annihilation flight factor as a function of energy.

Energy (MeV)	Born result	Seltzer's result	%Diff. Seltzer	AOMS result	Our Model	%Diff. Our Model
100.00	0.01127	0.01159	2.84	0.01059	0.01092	3.05
50.000	0.01858	0.01913	2.96	0.01735	0.01795	3.12
20.000	0.03034	0.03142	3.56	0.02840	0.02934	3.70
10.000	0.03743	0.03865	3.26	0.03503	0.03626	3.58
5.0000	0.03914	0.04042	3.27	0.03680	0.03814	3.69
2.0000	0.03232	0.03332	3.09	0.03040	0.03150	3.66
1.0000	0.02280	0.02346	2.89	0.02140	0.02214	3.44
0.5000	0.01336	0.01370	2.54	0.01250	0.01289	3.08
0.2000	0.00519	0.00529	1.93	0.00483	0.00494	2.39
0.1000	0.00228	0.00231	1.32	0.00211	0.00215	2.02
0.0500	0.00097	0.00098	1.03	0.00089	0.00091	1.10
0.0200	0.00032	0.00032	0.00	0.00023	0.00024	4.17

4.6 CALCULATION OF THE MASS ENERGY-ABSORPTION COEFFICIENT

The contribution of SQA to the mass energy-absorption coefficient is through the annihilation flight factor, as explained in Sections 3.2, 3.3 and 3.4. We notice that there is an increase of approximately 4% (see Table 4.3) in the annihilation flight factor when we include SQA. Therefore it is reasonable to conclude that its contribution to the photon mass energy-absorption coefficient will be larger. This conclusion comes from the fact that the calculation G_{pair} involves an integration of $\eta(T)$ (see equation (3.21).

CHAPTER 5

CONCLUSION

In this chapter the important results of the present calculation are reviewed.

We have derived a closed formula for the SQA K-shell cross section. The formula approximates well other results, though for low-Z elements ($Z < 47$) the formula has a poor approximation of the SQA cross section. The results of this formula are given in Figures 4.1 to 4.4.

The effect of binding-energy change on SQA cross sections (results from point-Coulomb[21]) has been analysed. It is seen that the SQA cross section increases at low energy. The contribution of the binding-energy change effect was calculated in the non-relativistic case. This was done in order to simplify the calculations. An exact relativistic calculation can be done by use of equation (2.43). This calculation would involve relativistic K-shell wave functions, and goes beyond the scope of this thesis.

K-shell total cross sections for heavy atoms are found to increase by several percents, as compared to the point-Coulomb values, when screening effects and binding-energy effects are included, and the increase is found to be largest for low positron energies (see Figures 4.5, 4.6, 4.7, and 4.8). In addition, the Z-dependence of the total cross section including binding-energy effects was found approximate to ($\sigma \sim Z^n$) be ~ 4.03.

The contribution of SQA to the value of photon mass energy-absorption coefficients has been calculated. This was achieved by calculating the contribution of SQA to the annihilation flight factor, equation (3.19). The contribution of SQA to the annihilation flight factor is approximately 4%. Therefore, its contribution to the mass energy-absorption coefficient is larger than 4%.

REFERENCES

1. P. A. M. Dirac, Proc. Camb. Phil. Soc. **26** 361 (1930)
2. H. A Bethe, Proc. R. Soc. Lond. **150**, 129 (1935)
3. T. Mukoyama, H. Mazaki, and S. Shimizu, Phys. Rev. **20** 82 (1979)
4. C. O. Carroll, and R. F. O'Connell, **132**, 2540 (1963)
5. W. Heitler, *The Quantum Theory of Radiation*, 3rd ed.
   (Oxford U. P., London, 1954)
6. H. K. Tseng, and R. H. Pratt, Phys. Rev. **A7**,1423 (1973)
7. E. Fermi, and G. E. Uhlenbeck, Phys. Rev. **44**, 510 (1933)
8. K. W. Broda, and W. R. Johnson, Phys. Rev. **A6**, 1693 (1972)
9. J. C. Jaeger, and H. R. Hulme, Proc. Camb. Philos. Soc. **32**, 158 (1936)
10. C. V. Sheth, and N. V. V. J. Swamy, Phys. Rev. **167**, 319 (1968)
11. W. R. Johnson, Phys. Rev. **159**, 61 (1967)
12. D. S. Moroi, A. Davidz, and R. F. Kess, Phys. Rev. **1**, 1647 (1970)
13. S. M. Seltzer, Radiation Research, **136**, 147 (1993), see also R. T. Berger, Radiation Research **15**, 1-29 (1961), J. H. Hubbell, NSRDS-NBS 29 (1969) and J. H. Hubbell, Nirmal Singh, B. Chand, D. Mehta, M. L. Garg, R. R. Garg, Surinder Singh and S. Puri, J. Phys. Chem. Ref. Data, Vol. **23**, No. 2, 1994, in J. H. Hubbell and Seltzer, NISTIR 5632 (1995) and in J. H. Hubbell, H. A. Gimm, and I. Overbo J. Phys. Chem. Ref. Data, Vol. **9**, No. 4 1980
14. G. Basbas, W. Brandt, and R. Laubert, Phys. Rev. **A7**, 983 (1973)

15. C. V. Sheth, Phys. Rev. **29**, 1151 (1984)

16. C. V. Sheth, Part of Ph.D. Thesis (unpublished)

17. G. Elwert, Ann. Phys. **34**, 178 (1939)

18. H. K. Tseng, and R. H. Pratt, Phys. Rev. **A4**, 1835 (1971)

19. Numerical Recipes, *The Art of Scientific Computing* (FORTRAN version) Cambridge University Press 1986. Editors: W. H. Press, B. P. Flannery, S. A. Teukolsky, and W. T. Vetterlung

20. R. H. Pratt and H. K. Tseng, Phys. Rev. **A5**, 1063 (1971)

21. W. R. Johnson, D. J. Buss, and C. O. Carroll, Phys. Rev. **135**, A1232 (1964)

22. J. C. Palathingal, P. Asoka-Kumar, K. G. Lynn, Y. Posada, and X. Y. Wu, Phys. Rev. **A51**, 2122 (1995)

23. M. J. Berger and S. M. Seltzer, *Stopping powers and Ranges of Electrons and Positrons*, Publication NBSIR 82-2550-A, National Bureau of Standards, Gaitherburg, MD. 1982.

24. J. H. Hubbell, W. J. Veigele, E. A. Briggs, R. T. Brown, D. T. Cromer, and R. J. Howerton, J. Phys. and Chem. Reference Data **4**, 471 (1975) and D. Schaupp, M. Schumacher, F. Smend, P. Rullhuson and J. H. Hubbell, J. Phys. Chem. Ref. Data, Vol. 12, 467, 1983.

25. Reference 23. pp 28

26. H. K. Tseng, and R. H. Pratt, Phys. Rev. **A3**, 100 (1970)

27. P. M. Bergstorm, Jr. , Lynn Kissel, and R. H. Pratt, Phys. Rev. **53** 2865 (1996)

28. *Handbook of Mathematical Functions*, National Bureau of Standards, M. Abramiwitz, editor.

29. M. E. Rose, *Elementary Theory of Angular Momentum*, Wiley, (1951)

30. H. J. Bhabha and H. R. Hulme, Proc. Roy. Soc. (London) **A146**, 723 (1934)

31. R. H. Pratt, Phys. Rev. **123**, 1508 (1961)

32. Banarjee, Nuovo Cimento, Vol. 11, No. 2, (1958), p. 220.

33. J. J. Sakurai, *Advanced Quantum Mechanics* (Addision - Wesley, New York, 1968) pp 140 - 143.

34. H. A. Bethe and E. E. Salpeter, *Quantum Mechanics Of One and Two Electron Atoms* (Academic Press Inc., New York, 1957)

35. J. Hubbell, Int. J. Appl. Radiat. Isot. Vol. 33 1269 (1982)

36. J. C. Slater, Phys. Rev. **81**, 3 (1951).

37. F. C. Smith and W. R. Johnson, Phys. Rev. **160**, 136 (1967).

38. P. D. Higgins, F. H. Attix, J. H. Hubbell, S. M. Seltzer, M. J. Berger, and C. H. Sibata, Publication NISTIR 4812, NIST, Gaitherburgy, MD, 1992.

39. M. J. Berger and J. H. Hubbell, XCOM: Photon Cross Sections on a Personal computer. Publication NBSIR 87-3597, National Bureau Of Standards, Gaitherburg, MD, 1987.

40. K. H. Spring, *Photons and Electrons*, Methuens and Co. Ltd, 1950. pp 85

41. W. Greiner, *Relativistic Quantum Mechanics,* Wave Equations, (Springer-Verlag, Berlin, 1990). pp 178-184.

42. T. Mukoyama and L. Sarkadi, Phys. Rev. **A3**, 1411 (1982).

43. J. H. Hubbell, Radiat. Phys. Chem. Vol. 50. No. 1, 113-124 (1997)

APPENDIX

COMPUTER PROGRAMS

APP.1: This program (program CROSS) gives the approximate SQA cross sections for various elements, Z = 47 to 90 according to the following equation

$$\sigma(W) = \frac{4\pi r_0^2 Z(Z\alpha)^4}{3(W^2-1)^{\frac{1}{2}}(W+1)^2} \frac{\beta\left(1-\exp\left(-\frac{2\pi\alpha Z}{\beta}\right)\right)}{\left(1+\frac{2\pi\alpha Z}{\beta}\right)}(3W^2+2W+4)$$
$$-\frac{W^2\log\left(W+(W^2-1)^{\frac{1}{2}}\right)}{(W+1)^4(W^2-1)^{\frac{1}{2}}} + \frac{(\alpha Z)^2 W^2}{(W+1)^7(W^2-1)^{\frac{1}{2}}}. \qquad \text{(A.1)}$$

This is equation (2.37) in Chapter 2.

APP.2: This program calculates the annihilation flight factor. The stopping power and radiative yields are obtained from reference 23. The main program is FLIGHT. The annihilation flight factor is defined as

$$\eta(T_0) = \frac{1}{T_0}\int_0^{T_0} W(T,T_0)T[1-Y(T)]dT. \qquad \text{(A.2)}$$

This is equation (3.19) in Chapter 3.

The various subroutines used are:

KALK: This subroutine performs the integral in the exponential. The quantities xc and yc are the values of the energy and the values of the annihilation probability (equation (3.6)). a and b are the limits of integration. The other quantities are defined in the program.

GAUSS: This subroutine evaluates the integrals in equation (3.19) numerically. fa and fb are the interpolated values of the quantities to be evaluated. a and b are the limits of integration and ss is the value of the integral that is returned by the subroutine.

RATINT: This subroutine is used for interpolation of the various arrays of values. The details of the various symbols are defined in the routine itself.

ABSCIS: This subroutine calculates the abscissas at which the integral in the exponential is to be evaluated. The points calculated by this routine are used for integration as lower limits for the integral in the exponential. These are calculated in a "random" manner and we use the routine shell to sort them in a ascending order.

SHELL: This routine sorts an array of values calculated by the routine abscis. The details about the various symbols are given in the routine itself.

APP.3: The main program is BIND. This program calculates the effect of binding-energy change on the point-Coulomb cross sections. The calculation is done in the non-relativistic case as explained in Chapter 2. These cross sections are taken from reference 21.

APP.4: This part of the appendix gives some of the values of the test integral (equation (4.4)).

NOTE: All computer programs are written in FORTRAN 77.

APP.1

* PROGRAM CROSS SECTION

```
      PROGRAM CROSS
      Character*30 ful
*     This program gives the correct approximate values for the sqa cross
*     sections for elements Z=47 to 90; equation (2.37).
      Parameter (alp = 1./137.,ro = 0.0793982,pi = 3.141593)
      Print*,'enter input file name'
      Read(*,*) ful
      Open(4,file = ful)
      Print*,'enter atomic number'
      Read(*,*) z
      Open(5, file = 'bus',status =' unknown')
      Coef=((4.*pi*ro*(z**5))*((alp)**4))
      Do 40 j = 1, 20
      Read(4,*)w, crss
      W2 = w**2
      Dow = 1./w2
      Beta = sqrt((1.-dow))
      Beta2 = beta**2
      Cop = (2.*pi*alp*z)/beta
      Top = beta*(1+exp(-cop))
      Deno = (1+cop)
      Rot = top/deno
      Smw = ((w+1.)**2)*(sqrt(w2-1.))
      Smw1 = ((w+1.)**4)*(sqrt(w2-1.))
      Smw2 = ((w+1.)**7)*(sqrt(w2-1.))
      Tem = (w2+(1./3.)*w+(4./3.))/smw
      Tam = w2*log(w+sqrt(w2-1))/smw1
      Tim = w2*((z*alp)**2)/smw2
      Sqa = coef*rot*tem-tam+tim
      Write(5,*)w,sqa,crss
40    continue
      Stop
      End
```

APP.2

```
*     PROGRAM ANNIHILATION FLIGHT FACTOR
      PROGRAM FLIGHT
*     This program calculates the annihilation flight factor. No analytic
*     formula is used for the stopping power and radiative
*     yield except for the cross section.  In this calculation the
*     2-quantum annihilation formula is used.  We add to the
*     cross section the contribution from 1-quantum annihilation.
      Parameter(n=65)
      Dimension xc(n),yc(n),y(n),dz(10)
      Dimension xint(10),wen(n),ohm(n)
      Open(2,file='lim')
      Open(3,file='radyld')
      Open(4,file='pstop.dat')
      Open(5,file='xint.dat')
      Open(6,file='ffact',status='unknown')
      Do 11 j=1,n
      Read(4,*)wen(j),ohm(j)
      Read(3,*)y(j)
      Xc(j)=wen(j)
      Yc(j)=wen(j)*(1.-y(j))*ohm(j)
11    continue
      Do 45 mn=1,12
      Read(2,*)t0,b,et
      Do 72 j=1,10
      Dz(j)=0.0
72    continue
      Call abscis(wen,ohm,dz,t0,n,xint)
      A=xc(1)
      Call kalk(xc,yc,xint,a,t0,n,sum)
      Sum=(sum/t0)
      Dif=100.*(abs(sum-et))/et
      Write(6,*)t0,b,et,sum
45    continue
      Stop
      End

      SUBROUTINE KALK(xc,yc,xint,a,b,nn,res)
      Dimension x(5),xa(65),ya(65),fa(5),fb(5),xc(nn),yc(nn)
      Dimension nri(5),nrf(5),xint(10)
      Data x/.1488743389,.4333953941,.6794095682,.8650633666,
     + .9739065285/
      Data nri/1,17,36,49,57/nrf/17,36,49,57,65/
      Xm=0.5*(b+a)
```

```
      Xr=0.5*(b-a)
      Ss=0.0
      Do 11 j=1,5
      ss=ss+w(j)*(fa(j)*exp(-xint(j+5))+fb(j)*exp(-xint(6-j)))
11    continue
      Ss=xr*ss
      Return
      End

      SUBROUTINE RATINT(xa,ya,n,x,y,dy)
*     Given arrays xa and ya, each of length n, and given a
*     value of x, this routine returns a value of y and an accuracy
*     estimate dy. The value returned is that of the diagonal rational
*     function, evaluated at x, which passes through the n points (xa_i, ya_i),
*     i=1,....,n.
      Parameter(nmax=65,tiny=1.e-25)
      Dimension xa(n),ya(n),c(nmax),d(nmax)
      Ns=1
      Hh=abs(x-xa(1))
      Do 11 i=1,n
      H=abs(x-xa(i))
      If(h.eq.0.)then
      Y=ya(i)
      Dy=0.0
      Return
      Else if(h.lt.hh)then
      Ns=i
      Hh=h
      End if
      C(i)=ya(i)
      D(i)=ya(i)+tiny
11    continue
      Y=ya(ns)
      Ns=ns-1
      Do 13 m=1,n-1
      Do 12 i=1,n-m
      W=c(i+1)-d(i)
      H=xa(i+m)-x
      T=(xa(i)-x)*d(i)/h
      Dd=t-c(i+1)
      If(dd.eq.0.)pause
      Dd=w/dd
      D(i)=c(i+1)*dd
      C(i)=t*dd
12    continue
```

```
      If(2*ns.lt.n-m)then
      Dy=c(ns+1)
      Else
      Dy=d(ns)
      Ns=ns-1
      End if
      Y=y+dy
13    continue
      Return
      End

      SUBROUTINE ABSCIS(xc,yc,dz,b,n,xint)
      Dimension xc(65),yc(65),adx(10),x(5),xint(10),dz(10)
      Data x/.1488743389,.4333953941,.6794095682,.8650633666,
     + .9739065285/
      A=xc(1)
      Xm=0.5*(b+a)
      Xr=0.5*(b-a)
      Jl=1
      Do 12 j=1,5
      Dx=xr*x(j)
      Adx(jl)=xm+dx
      Jl=jl+1
      Adx(jl)=xm-dx
      Jl=jl+1
12    continue
      Kk=10
      Call shell(kk,adx)
      Do 50 i=1,10
      A=adx(i)
      Call kalk(xc,yc,dz,a,b,n,sum)
      Xint(i)=sum
50    continue
      Return
      End

      SUBROUTINE SHELL(n,arr)
*     This routine sorts an array arr of length n into ascending numerical
*     order, by the Shell-Mezgar algorithm (diminishing increment sort) n
*     is input; arr is replaced by an output its sorted rearrangement.
*     Parameter(aln2i=1.4426952,tiny=1.e-5)
      Dimension arr(10)
      Lognb2=int(alog(float(n))*aln2i+tiny)
      M=n
      Do 12 nn=1,lognb2
```

```
      M=m/2
      K=n-m
      Do 11 j=1,k
      I=j
3     continue
      L=i+m
      If(arr(l).lt.arr(i))then
      T=arr(i)
      Arr(i)=arr(l)
      Arr(l)=t
      I=i-m
      If(i.ge.1)go to 3
      Endif
11    continue
12    continue
      Return
      End
```

APP.3

```
*     PROGRAM BINDING ENERGY CHANGE
      PROGRAM BIND
      Dimension w(3),ww(3),wqd(3)
      parameter(r=13.6,alp=1./137.0,v0=2.19e+6,c=3.0e+8)
      data ww/542.941,574.878,606.816/
*     This program does the calculation of the binding effect
*     on the sqa cross section. We use the point coulomb sqa
*     cross sections given by Johnson et al[21]. The result is quiet
*     significant for low energy.
      print*,'enter z and sigma squared'
      read(*,*)z, sigma
      u=(1.-sqrt(1.-(alp*z)**2))*511003.
      do 10 j=1,3
      w(j)=1.+ww(j)/511.003
      wqd(j)=w(j)**2
      dow=1./wqd(j)
      v1=c*sqrt(1.-dow)
      z2k=z-0.3
      z2k2=z2k**2
      etak=((v1/v0)**2)/z2k2
      thetak=u/(z2k2*r)
      zaik=2.*sqrt(etak)/thetak
      gg=g(zaik)
      eta=1.+(2./(z2k*thetak))*gg
      beng=eta*u
      dif=(beng-u)/511003.
      write(*,*)ww(j),eta,dif
10    continue
      stop
      end

      FUNCTION g(x)
      cof=(1.+x)**(-5)
      x2=x**2
      x3=x**3
      x4=x**4
      g=cof*(1.+5.0*x+7.14*x2+4.27*x3+0.947*x4)
      return
      end
```

APP.4

In this appendix we give some of numerical and analytical results of the integral

$$\mathrm{Int} = \int_0^{x_0} y \exp\left(-\int_y^{x_0} y' \, dy' \right) dy . \tag{A.3}$$

For example some of the results of this integral are

X_0	Numerical	Analytical
1.0	0.39211	0.39347
2.0	0.85943	0.86466
4.0	0.99786	0.99962